

Investigating and Mitigating the Side Effects of Noisy Views in Multi-view Clustering in Practical Scenarios

Jie Xu, Gang Niu, Xiaolong Wang, Yazhou Ren, Lei Feng, Xiaoshuang Shi, Heng Tao Shen, Xiaofeng Zhu

Abstract

Multi-view clustering (MvC) aims at exploring the category structure among multi-view data without label supervision. Multiple views provide more information than single views and thus existing MvC methods can achieve satisfactory performance. However, their performance might seriously degenerate when the views are noisy in practical scenarios. In this paper, we first formally investigate the drawback of noisy views and then propose a theoretically grounded deep MvC method (namely MvCAN) to address this issue. Specifically, we propose a novel MvC objective that enables un-shared parameters and inconsistent clustering predictions across multiple views to reduce the side effects of noisy views. Furthermore, a non-parametric iterative process is designed to generate a robust learning target for mining multiple views' useful information. Theoretical analysis reveals that MvCAN works by achieving the multi-view consistency, complementarity, and noise robustness. Finally, experiments on public datasets demonstrate that MvCAN outperforms state-of-the-art methods and is robust against the existence of noisy views.

1. Introduction

In real-world scenarios, a common phenomenon is that one sample can be described by multiple views, as known as multi-view data. Multi-view clustering (MvC) can recognize the category patterns hidden in multi-view data without the label supervision and has been attracting increasing attention (Bickel & Scheffer, 2004). In the literature, MvC could be roughly divided into two groups including traditional methods (Wen et al., 2018; Liu et al., 2018; Li et al., 2019a; Yang et al., 2021) and deep methods (Abavisani & Patel, 2018; Huang et al., 2020; Pan & Kang, 2021; Trosten et al., 2021), and we conduct a detailed review in Appendix A.

Jie Xu, Xiaolong Wang, Yazhou Ren, Xiaoshuang Shi, Heng Tao Shen, and Xiaofeng Zhu are with University of Electronic Science and Technology of China. Gang Niu is with Center for

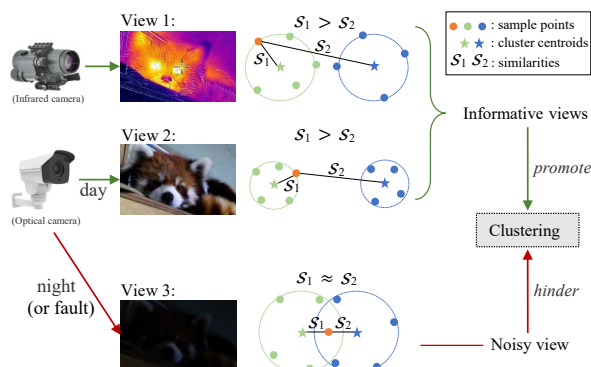


Figure 1. Illustration of the noisy-view drawback (NVD). The informative views have distinct representation similarities, which can promote clustering due to their consistency and complementarity. However, the noisy views have indistinct representation similarities. For instance, the views extracted from faulty or inapplicable sensors will bring noisy information and hinder clustering, making it be of practical significance to investigate the noise robustness.

The success of existing MvC methods lies in that they are able to explore the *consistency* and *complementarity* among multi-view data (Bickel & Scheffer, 2004; Zhao et al., 2017; Zhang et al., 2019), thereby outperforming single-view clustering (SvC) methods (MacQueen, 1967; Ng et al., 2001; Xie et al., 2016). The consistency indicates that multiple views have the consistent information which is helpful for recognizing the same category (Tzortzis & Likas, 2012; Cao et al., 2015; Zhan et al., 2018). The complementarity means that different views contain the complementary information which is conducive to reciprocally correcting and supplementing each other (Xu et al., 2021; Du et al., 2022; Yang et al., 2022). Consistency and complementarity of multiple views are abstract concepts, to explore them, the most popular manner of previous works utilizes fusion strategies to learn the common representations and consistent clustering predictions for all views (Wang et al., 2019; Zhan et al., 2019; Zhou & Shen, 2020; Wen et al., 2020; Trosten et al., 2021; Liu et al., 2021; Wang et al., 2021). For instance, Wang et al. (2019) achieved the multi-view consistency in the consensus clustering partition via late fusion alignment. Zhou & Shen (2020) explored the multi-view

Advanced Intelligence Project, RIKEN, Japan. Lei Feng is with Chongqing University.

complementarity with attention mechanisms and conducted unified clustering among the fused representations.

Despite important advance, experiments show that MvC is not necessarily better than SvC, due to that the samples' features extracted from some views could be noisy that might have useless even harmful information for clustering. For an example shown in Figure 1, considering animals at night, the view from infrared cameras is informative, but the view from optical cameras is noisy. Compared with informative views, noisy views play a negative role in identifying the common category in multi-view clustering. In a multi-view dataset, the more samples with noisy views, the more side effects of noisy views. This phenomenon has been rarely investigated so far and this paper shortly entitles it Noisy-view Drawback (NVD). There are two reasons that the NVD negatively affects the performance of existing MvC methods. First, previous works usually learn the representations by fusing multiple views, whereas the parameters in the established fusion modules are shared by all views (Wang et al., 2016; Zhang et al., 2017; Zhou et al., 2019; Wang et al., 2019; Liu et al., 2021). Because the clustering objective punished on the noisy view might be dominant that on other informative views, causing the shared parameters to fit the noisy view and thus missing the useful information of other views. Second, many methods tend to obtain consistent clustering predictions for all views (Nie et al., 2016; Wang et al., 2018; Zhan et al., 2019; Zhou & Shen, 2020; Tang & Liu, 2022a). Nevertheless, it is unreasonable to force the clustering prediction of the noisy view to be the same as that of other views, inversely, this process might make the learning and clustering on the informative views degenerate.

In this paper, we consider the NVD and propose a theoretically grounded deep MvC method termed MvCAN: *Multi-view Clustering Against Noisy-view Drawback*. Firstly, based on the aforementioned two reasons, the proposed clustering objective requires the un-shared parameters for all views and optimizes a subproblem that allows inconsistent clustering predictions among individual views. Therefore, MvCAN designs the parameter-decoupled deep model of learning representations and clustering predictions for each view, aiming to avoid the side effects of noisy views. Secondly, MvCAN establishes a non-parametric iterative process to output a robust learning target for training the model. To be exact, the non-parametric iterative process infers scaling factors for multiple views to automatically recognize their informative levels, which makes MvCAN can explore the useful information among informative views and be robust to noisy views. Finally, a bi-level optimization strategy is proposed to make learning representations and clustering promote each other. Different from previous works, this work has the following contributions:

- The NVD is pervasive but challenging in multi-view clustering, which motivates us to research the robust-

ness towards noisy views. To this end, we propose a novel clustering objective that uses un-shared parameters and does not require consistent clustering predictions for all views, to eliminate the adverse interference between the noisy views and the informative views.

- In the literature, rare works theoretically describe the consistency and complementarity of multi-view learning. This paper attempts to theoretically investigate the consistency and complementarity relations among multiple views, and explain the achieved noise robustness.
- Within a bi-level optimization strategy, we propose a non-parametric iterative process that generates iterative robust learning targets to train the deep model. The evaluations on public datasets and their noise-simulated versions demonstrate the superior performance of our MvCAN over the SOTA methods.

2. Background and Analysis

Notations. $\{\mathbf{X}^v \in \mathbb{R}^{N \times D_v}\}_{v=1}^V$ denotes a multi-view dataset which contains N samples with V views. $\mathbf{Z}^v \in \mathbb{R}^{N \times d_v}$ and $\mathbf{Y}^v \in \mathbb{R}^{N \times K}$ denote the learned representations and soft labels in the v -th views. D_v and d_v denote the dimensionality of \mathbf{X}^v and \mathbf{Z}^v . K is the cluster number. Table 5 in Appendix A lists the details of all used notations.

2.1. Preliminaries

Deep embedded clustering, *i.e.*, DEC (Xie et al., 2016), is a SvC method that provides an impressive optimization paradigm to promote the representation learning for clustering. Specifically, for a single view, DEC learns the representations \mathbf{Z} from data matrix \mathbf{X} and conducts end-to-end clustering by learning the soft labels \mathbf{Y} based on \mathbf{Z} , with the trainable cluster centroids $\{\boldsymbol{\mu}_j\}_{j=1}^K$ in representation space:

$$y_{ij} = \frac{(1 + \|\mathbf{z}_i - \boldsymbol{\mu}_j\|_2^2)^{-1}}{\sum_{j=1}^K (1 + \|\mathbf{z}_i - \boldsymbol{\mu}_j\|_2^2)^{-1}} \in \mathbf{Y}, \quad (1)$$

where $\mathbf{z}_i = \mathcal{E}_{\Phi}(\mathbf{x}_i) \in \mathbf{Z}$ is the new representation of the i -th sample $\mathbf{x}_i \in \mathbf{X}$, obtained by the deep encoder network \mathcal{E}_{Φ} with the parameters Φ . $(1 + \|\mathbf{z}_i - \boldsymbol{\mu}_j\|_2^2)^{-1}$ can be interpreted as the representation similarity in Definition 3.1. We have $\sum_j y_{ij} = 1$ and y_{ij} represents the probabilistic soft label indicating that the sample \mathbf{x}_i comes from the j -th cluster. Then, DEC establishes the learning target $\mathbf{T} \in \mathbb{R}^{N \times K}$ to refine \mathbf{Y} by training the model parameters, where

$$t_{ij} = \frac{(y_{ij})^2 / \sum_{i=1}^N y_{ij}}{\sum_{j=1}^K \left((y_{ij})^2 / \sum_{i=1}^N y_{ij} \right)} \in \mathbf{T}. \quad (2)$$

Indeed, Eq. (2) enhances the elements of large values in the soft labels \mathbf{Y} for each sample. As a result, this learning

paradigm establishes the learning target \mathbf{T} to push the soft labels \mathbf{Y} to learn the cluster structures with high confidence.

2.2. Analysis of Noisy-view Drawback (NVD)

The aforementioned learning paradigm inspires a lot of developments and is one of the most widely used approaches to conduct deep MvC (Xu et al., 2019; Wen et al., 2020; Wang et al., 2021; Xie et al., 2020; Fan et al., 2020). For MvC, previous methods usually learn the representations \mathbf{Z}^v and soft labels \mathbf{Y}^v for individual views, and then leverage the fusion strategies to explore useful information hidden in multiple views, e.g., early fusion (Wen et al., 2020; Wang et al., 2021) and late fusion (Xie et al., 2020). They also construct the learning target \mathbf{T} with Eq. (2) to train models.

Although some efforts (Wen et al., 2020; Trosten et al., 2021; Wang et al., 2021) consider the view diversity and propose weighting strategies in fusion modules, previous methods usually leverage shared parameters and consistent clustering predictions for multiple views, whose models might be not robust when there are low-quality even noisy views in practical scenarios (which will be verified in Section 4.2). To illustrate this, we denote $\{\mathbf{Z}^v\}_{v=1}^V$ as all views' representations and consider an ideal clustering objective:

$$\min_{\Theta} \sum_{v=1}^V \|\mathbf{T} - \mathcal{F}_{\Theta}(\mathbf{Y}^v | \{\mathbf{Z}^v\}_{v=1}^V)\|_F^2, \quad (3)$$

where we write $\mathbf{Y}^v = \mathcal{F}_{\Theta}(\mathbf{Y}^v | \{\mathbf{Z}^v\}_{v=1}^V)$ through the fusion module \mathcal{F} and Θ denotes the set of parameters shared by all V views. \mathbf{T} is the unified learning target for training the consistent soft labels $\{\mathbf{Y}^v\}_{v=1}^V$ of all views. With the ground-truth label matrix $\mathbf{L} \in \{0, 1\}^{N \times K}$, we further have the following theorem to indicate the relationship between clustering effectiveness and views' clustering objectives:

Theorem 2.1. Denoting $\check{\mathbf{Y}} = \mathbf{L}\mathbf{A}$, where $\mathbf{A} \in \{0, 1\}^{K \times K}$ makes $\check{\mathbf{Y}}$ maximally match the learning target \mathbf{T} . Then, the clustering accuracy can be calculated as $ACC = \frac{1}{N} (N - \frac{1}{2} \|\check{\mathbf{Y}} - \mathbf{T}\|_F^2) = 1 - \frac{1}{2N} \|\check{\mathbf{Y}} - \mathbf{T}\|_F^2$. In Eq. (3), if Θ is shared by multiple views and their soft labels $\{\mathbf{Y}^v\}_{v=1}^V$ have consistent learning target \mathbf{T} , we have

$$ACC \leq 1 - \frac{1}{2N} \left(\max_{1 \leq m \leq V} \|\check{\mathbf{Y}} - \mathcal{F}_{\Theta}(\mathbf{Y}^m | \{\mathbf{Z}^v\}_{v=1}^V)\|_F^2 - \|\mathbf{T} - \mathcal{F}_{\Theta}(\mathbf{Y}^v | \{\mathbf{Z}^v\}_{v=1}^V)\|_F^2 \right). \quad (4)$$

Specifically, we denote $m^* = \arg \max_{1 \leq m \leq V} \|\check{\mathbf{Y}} - \mathcal{F}_{\Theta}(\mathbf{Y}^m | \{\mathbf{Z}^v\}_{v=1}^V)\|_F^2$ and $\|\check{\mathbf{Y}} - \mathcal{F}_{\Theta}(\mathbf{Y}^{m^*} | \{\mathbf{Z}^v\}_{v=1}^V)\|_F^2$ could reflect the largest clustering loss $\|\mathbf{T} - \mathcal{F}_{\Theta}(\mathbf{Y}^{m^*} | \{\mathbf{Z}^v\}_{v=1}^V)\|_F^2$, corresponding to the view with the worst quality (or even the noisy view). No matter how the set of parameters Θ is optimized, for the m^* -th view, the unclear cluster structures and inherent noise properties of \mathbf{Z}^{m^*} make it difficult for \mathbf{Y}^{m^*} to fit

the learning target \mathbf{T} . Therefore, the noisy view has a large clustering loss that is difficult to minimize, i.e., $\|\mathbf{T} - \mathcal{F}_{\Theta}(\mathbf{Y}^{m^*} | \{\mathbf{Z}^v\}_{v=1}^V)\|_F^2$, which usually dominates the optimization of other views in Eq. (3). This makes the shared parameters Θ tend to fit the noisy view, resulting the model degeneration on other views which have the small clustering losses that are easy to minimize, e.g., $\sum_{v \neq m^*} \|\mathbf{T} - \mathcal{F}_{\Theta}(\mathbf{Y}^v | \{\mathbf{Z}^v\}_{v=1}^V)\|_F^2$. As a consequence, the noisy view will limit the clustering effectiveness due to the upper bound in Eq. (4).

3. Methodology

3.1. MvCAN: Multi-view Clustering Against Noisy-view Drawback

To alleviate the NVD, we propose MvCAN whose multi-view clustering objective should consider the following two conditions. The first condition is that we require the parameters to be decoupled for all views instead of using fusion modules as previous works. The second condition is that we allow different views to have different clustering predictions in training instead of consistent ones as previous works.

Accordingly, we propose a novel multi-view clustering objective (denoted by \mathcal{L}_c) as follows:

$$\begin{aligned} \mathcal{L}_c : & \min_{\{\Theta^v\}_{v=1}^V} \min_{\{\mathbf{A}^v\}_{v=1}^V} \sum_{v=1}^V \|\mathbf{T}\mathbf{A}^v - \mathcal{F}_{\Theta^v}^v(\mathbf{Y}^v | \mathbf{Z}^v)\|_F^2 \\ \text{s.t.} & p(\Theta^a, \Theta^b) = p(\Theta^a)p(\Theta^b), a, b \in \{1, 2, \dots, V\}, a \neq b, \\ & \mathbf{A}^v (\mathbf{A}^v)^T = \mathbf{I}_K, \mathbf{A}^v \in \{0, 1\}^{K \times K}, \end{aligned} \quad (5)$$

where we write $\mathbf{Y}^v = \mathcal{F}_{\Theta^v}^v(\mathbf{Y}^v | \mathbf{Z}^v)$ whose calculation follows Eq. (1). $\mathbf{Z}^v = \mathcal{E}_{\Phi^v}^v(\mathbf{X}^v)$ and $\mathcal{E}_{\Phi^v}^v$ denotes the encoder of individual view. The two conditions in Eq. (5) are specifically illustrated as follows:

Condition 1: In this framework, the set of parameters Θ^v includes $\{\mu_j^v\}_{j=1}^K$ and Φ^v of the v -th view. We leverage $p(\Theta^a, \Theta^b) = p(\Theta^a)p(\Theta^b)$ to indicate that $\{\Theta^v\}_{v=1}^V$ are un-shared for each other, so as to avoid the limitations caused by the NVD analyzed in Section 2.2. This condition designs the parameter-decoupled model of learning representations $\{\mathbf{Z}^v\}_{v=1}^V$ and clustering predictions $\{\mathbf{Y}^v\}_{v=1}^V$ for each view, aiming to eliminate the dominated influence of noisy views on informative views.

Condition 2: Before training the parameters $\{\Theta^v\}_{v=1}^V$, we solve a subproblem in optimizing the clustering objective \mathcal{L}_c , i.e., $\min_{\{\mathbf{A}^v\}_{v=1}^V} \sum_{v=1}^V \|\mathbf{T}\mathbf{A}^v - \mathcal{F}_{\Theta^v}^v(\mathbf{Y}^v | \mathbf{Z}^v)\|_F^2$, which makes $\sum_{v=1}^V \|\mathbf{T}\mathbf{A}^v - \mathcal{F}_{\Theta^v}^v(\mathbf{Y}^v | \mathbf{Z}^v)\|_F^2 \leq \sum_{v=1}^V \|\mathbf{T} - \mathcal{F}_{\Theta^v}^v(\mathbf{Y}^v | \mathbf{Z}^v)\|_F^2$. For each view, this subproblem is equivalent to $\min_{\mathbf{A}^v} \|\mathbf{T}\mathbf{A}^v - \mathbf{Y}^v\|_F^2$ in which $\mathbf{A}^v \in \{0, 1\}^{K \times K}$ achieves the maximum match between the learning target \mathbf{T} and the soft labels \mathbf{Y}^v . This condition makes the clustering loss smaller for each view, as well as considers that it does

not make sense to learn consistent clustering predictions for both informative views and noisy views.

In brief, to overcome the side effects of noisy views, MvCAN does not adopt the previous popular fusion strategies and allows inconsistent clustering predictions for multiple views, but how can Eq. (5) explore the useful consistent and complementary information from multiple views? To this end, we propose a non-parametric iterative process to generate the robust learning target \mathbf{T} for optimizing Eq. (5).

The proposed non-parametric iterative process indicates that its computation will not change the parameters $\{\Theta^v\}_{v=1}^V$. In each iteration of the process, we design the scaling matrix $\mathbf{W}_{(t)}$ to automatically explore the informative levels of the views for obtaining the scaled representation $\mathbf{Z}_{(t)}$, and then produce the robust soft labels $\mathbf{Y}_{(t)}$. The theoretical analysis in Section 3.3 demonstrates that $\mathbf{Y}_{(t)}$ achieve the consistency and complementarity across multiple views, as well as the noise robustness for the noisy views.

Concretely, in the t -th iteration, the proposed MvCAN infers the scaled representations $\mathbf{Z}_{(t)} \in \mathbb{R}^{N \times \sum_v d_v}$ from all views by the multiplication between the representations $[\mathbf{Z}^1 \ \mathbf{Z}^2 \ \dots \ \mathbf{Z}^V] \in \mathbb{R}^{N \times \sum_v d_v}$ and the scaling matrix $\mathbf{W}_{(t)} \in \mathbb{R}^{\sum_v d_v \times \sum_v d_v}$:

$$\begin{aligned} \mathbf{Z}_{(t)} &= [\mathbf{Z}^1 \ \mathbf{Z}^2 \ \dots \ \mathbf{Z}^V] \mathbf{W}_{(t)} \\ &= [\mathbf{Z}^1 \ \mathbf{Z}^2 \ \dots \ \mathbf{Z}^V] \begin{bmatrix} w_{(t)}^1 \mathbf{I}^1 & & & \\ & w_{(t)}^2 \mathbf{I}^2 & & \\ & & \ddots & \\ & & & w_{(t)}^V \mathbf{I}^V \end{bmatrix}, \end{aligned} \quad (6)$$

where $\mathbf{W}_{(t)}$ is a block diagonal matrix ($\mathbf{W}_{(1)} = \mathbf{I}$), of which each block is the multiplication between the unit matrix $\mathbf{I}^v \in \{0, 1\}^{d_v \times d_v}$ and the scaling factor $w_{(t)}^v \in \mathbb{R}$ for the individual view. Based on the scaled representations $\mathbf{Z}_{(t)}$, MvCAN generates the robust soft labels $\mathbf{Y}_{(t)} \in \mathbb{R}^{N \times K}$ in the t -th iteration. To be specific, $\mathbf{Y}_{(t)}$ should reflect the cluster structures among $\mathbf{Z}_{(t)}$, and thus we leverage a variant of Eq. (1) to compute $\mathbf{Y}_{(t)}$. Concretely, $\mathbf{z}_{i(t)} \in \mathbf{Z}_{(t)}$ and we denote $\mathbf{Y}_{(t)} = \mathcal{F}'(\mathbf{Y}_{(t)}|\mathbf{Z}_{(t)})$:

$$y_{ij(t)} = \frac{(1 + \|\mathbf{z}_{i(t)} - \mathbf{c}_{j(t)}\|_2^2)^{-1}}{\sum_{j=1}^K (1 + \|\mathbf{z}_{i(t)} - \mathbf{c}_{j(t)}\|_2^2)^{-1}} \in \mathbf{Y}_{(t)}, \quad (7)$$

where $\{\mathbf{c}_{j(t)} \in \mathbb{R}^{\sum_v d_v}\}_{j=1}^K$ represent the cluster centroids of $\mathbf{Z}_{(t)}$ in the t -th iteration. Note that $\{\mathbf{c}_{j(t)}\}_{j=1}^K$ are computed by K -means (MacQueen, 1967) from the scratch in each iteration, it will not change the parameters $\{\Theta^v\}_{v=1}^V$. Furthermore, denoting I and H as mutual information and entropy, respectively, based on the normalized mutual information between the robust soft labels $\mathbf{Y}_{(t)}$ and the soft labels \mathbf{Y}^v of individual view, we formulate the iterative

Algorithm 1 : The bi-level optimization strategy

Input: Dataset $\{\mathbf{X}^v\}_{v=1}^V$, cluster number K , hyperparameter λ , iterations T_1 and T_2 , epoch E

Initialize parameters Φ^v and Ψ^v by Eq. (9) and initialize $\{\mu_j^v\}_{j=1}^K$ by K -means algorithm, $\mathbf{W}_{(1)} = \mathbf{I}$

for $e < E$ **do**

/ \mathcal{T} -level optimization leverages the learned representations to obtain the robust learning target*/*

for $t \in \{1, 2, \dots, T_1\}$ **do**

Update $\mathbf{Z}_{(t)} = [\mathbf{Z}^1 \ \mathbf{Z}^2 \ \dots \ \mathbf{Z}^V] \mathbf{W}_{(t)}$ by Eq. (6)

Update $\mathbf{Y}_{(t)} = \mathcal{F}'(\mathbf{Y}_{(t)}|\mathbf{Z}_{(t)})$ by Eq. (7)

Update $\mathbf{W}_{(t+1)}$ by Eq. (8)

Update $\mathbf{T} = \mathcal{T}(\mathbf{T}|\mathbf{Y}_{(t)})$ as Eq. (2)

/ \mathcal{R} -level optimization leverages the learning target to learn the clustering-oriented representations*/*

Compute \mathbf{A}^v by solving $\min_{\mathbf{A}^v} \|\mathbf{T}\mathbf{A}^v - \mathbf{Y}^v\|_F^2$ with Hungarian algorithm

for $t \in \{1, 2, \dots, T_2\}$ **do**

Update Φ^v , Ψ^v , and Θ^v by Eq. (10) with mini-batch Adam algorithm

$e = e + 1$

Compute cluster assignment by $\arg \max_j y_{ij}, y_{ij} \in \mathbf{Y}_{(t)}$.

strategy of the scaling matrix as:

$$w_{(t+1)}^v = \exp\left(\frac{2I(\mathbf{Y}^v; \mathbf{Y}_{(t)})}{H(\mathbf{Y}^v) + H(\mathbf{Y}_{(t)})}\right) \in \mathbf{W}_{(t+1)}. \quad (8)$$

Since the computations of $\mathbf{Y}_{(t)}$ and $\{\mathbf{Y}^v\}_{v=1}^V$ are all unsupervised, in effect, MvCAN can automatically recognize the informative levels of the views based on the mutual information among their soft labels, and then constrains their representations with different scaling factors, and then produces the robust soft labels $\mathbf{Y}_{(t+1)}$.

After finishing the iteration of $\mathbf{Y}_{(t)}$, we utilize Eq. (2) to obtain the robust learning target, written as $\mathbf{T} = \mathcal{T}(\mathbf{T}|\mathbf{Y}_{(t)})$. Thus, the robust learning target \mathbf{T} is based on the already learned representations and soft labels, *i.e.*, $\{\mathbf{Z}^v, \mathbf{Y}^v\}_{v=1}^V$. The iterative process outputs \mathbf{T} that is further leveraged to refine $\{\mathbf{Y}^v\}_{v=1}^V$ for all views as formulated in Eq. (5).

3.2. Loss Function and Optimization

We follow previous deep MvC methods (Xu et al., 2019; Xie et al., 2020; Fan et al., 2020; Wen et al., 2020; Wang et al., 2021) and adopt deep autoencoders to learn the new representations of multi-view data. Letting $\mathcal{E}_{\Phi^v}^v$ and $\mathcal{D}_{\Psi^v}^v$ respectively denote the encoder and decoder, our method requires that the parameters Φ^v and Ψ^v of each view are unshared for other views according to Condition 1. Therefore, for the v -th view, the reconstruction $\hat{\mathbf{X}}^v = \mathcal{D}_{\Psi^v}^v(\mathbf{Z}^v)$ is only related to $\mathbf{Z}^v = \mathcal{E}_{\Phi^v}^v(\mathbf{X}^v)$, and our representation learning objective (denoted by \mathcal{L}_r) can be formulated as follows:

$$\begin{aligned}
 \mathcal{L}_r : & \min_{\{\Psi^v, \Phi^v\}_{v=1}^V} \sum_{v=1}^V \|\mathbf{X}^v - \mathcal{D}_{\Psi^v}^v(\mathcal{E}_{\Phi^v}^v(\mathbf{X}^v))\|_F^2 \\
 \text{s.t. } & p(\Psi^a, \Psi^b) = p(\Psi^a)p(\Psi^b), p(\Phi^a, \Phi^b) = p(\Phi^a)p(\Phi^b) \\
 & a, b \in \{1, 2, \dots, V\}, a \neq b.
 \end{aligned} \tag{9}$$

In conclusion, the loss function to train the deep model of MvCAN includes the following two parts:

$$\mathcal{L} = \mathcal{L}_r + \lambda \mathcal{L}_c, \tag{10}$$

where λ achieves the trade-off between \mathcal{L}_r and \mathcal{L}_c . In the optimization of MvCAN, \mathcal{L}_r conducts the fundamental representation learning for individual views, and \mathcal{L}_c explores the cluster structures in the representations of multiple views. To make the representation learning and clustering promote each other, we propose a bi-level optimization strategy (\mathcal{T} - and \mathcal{R} -level) as shown in Algorithm 1 and Figure 6.

Convergence & Complexity. In \mathcal{T} -level optimization, K -means will be adopted to calculate the cluster centroids for $\mathbf{Z}_{(t)} \in \mathbb{R}^{N \times \sum_{v=1}^V d_v}$, which has a convex objective function with the complexity of $O(NK \sum_{v=1}^V d_v)$. Eqs. (2), (6), (7), and (8) only involve the computation process with the complexity of $O(N)$. In \mathcal{R} -level optimization, $\min_{\mathbf{A}^v} \|\mathbf{T}\mathbf{A}^v - \mathbf{Y}^v\|_F^2$ is a convex objective function and Hungarian algorithm has the complexity of $O(K^3)$. The loss function of Eq. (10) is also convex with the complexity of $O(N \sum_{v=1}^V d_v + VNK)$. Hence, both \mathcal{T} - and \mathcal{R} -level optimizations can converge, and the total complexity is $O(E/T_2(T_1(NK \sum_{v=1}^V d_v) + VK^3 + VNK))$ with respect to iterations T_1 and T_2 , epoch E , and data size N . The complexity to train deep autoencoders is also linear to N .

3.3. Theoretical Analysis of Multi-view Consistency, Complementarity, and Noise Robustness

Moreover, we attempt to theoretically illustrate why MvCAN works with the following definitions and theorems:

Definition 3.1. Denoting $\mathcal{D}(\mathbf{a}, \mathbf{b}) = \|\mathbf{a} - \mathbf{b}\|_2^2$ as squared Euclidean distance between the representations \mathbf{a} and \mathbf{b} ,

$$\mathcal{S}(\mathbf{a}, \mathbf{b}) := \frac{1}{1 + \mathcal{D}(\mathbf{a}, \mathbf{b})} \in (0, 1] \tag{11}$$

is defined as the representation similarity between \mathbf{a} and \mathbf{b} . Formally, $y_{ij}^v \in (0, 1]$ holds.

Letting μ_a^v and μ_b^v denote the a -th and the b -th cluster centroids in the representation space of \mathbf{Z}^v , $\mathbf{z}_i^v \in \mathbf{Z}^v$, we have $\mathcal{S}(\mathbf{z}_i^v, \mu_a^v) > \mathcal{S}(\mathbf{z}_i^v, \mu_b^v) \Rightarrow y_{ia}^v > y_{ib}^v$ and $\mathcal{S}(\mathbf{z}_i^v, \mu_a^v) < \mathcal{S}(\mathbf{z}_i^v, \mu_b^v) \Rightarrow y_{ia}^v < y_{ib}^v$, because

$$\begin{aligned}
 y_{ij}^v &= \frac{(1 + \|\mathbf{z}_i^v - \mu_j^v\|_2^2)^{-1}}{\sum_{j=1}^K (1 + \|\mathbf{z}_i^v - \mu_j^v\|_2^2)^{-1}} \\
 &= \frac{\mathcal{S}(\mathbf{z}_i^v, \mu_j^v)}{\sum_{j=1}^K \mathcal{S}(\mathbf{z}_i^v, \mu_j^v)} \propto \mathcal{S}(\mathbf{z}_i^v, \mu_j^v).
 \end{aligned} \tag{12}$$

Definition 3.2. ($\varepsilon, \mathbf{z}, \mu$ - Noisy-view) For $\forall \mathbf{z}_i^v \in \mathbf{Z}^v$, it belongs to the noisy view if $\exists \mu_a^v, \mu_b^v$, and $\varepsilon > 0$ such that $|\mathcal{D}(\mathbf{z}_i^v, \mu_a^v) - \mathcal{D}(\mathbf{z}_i^v, \mu_b^v)| < \varepsilon$, $\mathcal{S}(\mathbf{z}_i^v, \mu_a^v) \approx \mathcal{S}(\mathbf{z}_i^v, \mu_b^v)$, and $y_{ia}^v \approx y_{ib}^v$, where ε is a sufficiently small value. Otherwise, \mathbf{z}_i^v is the informative view.

Then, the following theorems indicate that, in the framework of MvCAN, $\mathbf{Y}_{(t)}$ achieves the consistency, complementarity, and noise robustness with regard to $\{\mathbf{Y}^v\}_{v=1}^V$. All the proofs of the following theorems are provided in Appendix B.

Theorem 3.3. Denoting \mathcal{L}_K as the K -means objective, $\mathcal{L}_K(\mathbf{Z}_{(t)})$ is equivalent to punishing different scaling factors on $\{\mathcal{L}_K(\mathbf{Z}^v)\}_{v=1}^V$ under the consistency constraint of multiple views' cluster centroids.

Theorem 3.3 analyses the effect of the scaling matrix $\mathbf{W}_{(t)}$ in the scaled representation $\mathbf{Z}_{(t)}$ to constrain the optimization of individual views, which reduces the effects of noisy views in discovering the cluster structures.

Theorem 3.4. (Consistency) If a sample representation is informative in multiple views and has the same cluster assignments in these views, its cluster assignment in $\mathbf{Y}_{(t)}$ is the same as that in these views.

Theorem 3.4 indicates that $y_{ij(t)} \in \mathbf{Y}_{(t)}$ follows $\{y_{ij}^v \in \mathbf{Y}^v\}_{v=1}^V$ when they have consistent clusters, which reflects the consistency of multiple views.

Theorem 3.5. (Complementarity) If a sample representation is informative in multiple views where it has different cluster assignments, we have two cases according to the differences of similarity among the clusters.

Case 1: if the differences of similarity among the clusters are equal, its cluster assignment in $\mathbf{Y}_{(t)}$ is the same as that in the informative view with the largest scaling factor.

Case 2: if the differences of similarity among the clusters are not equal, its cluster assignment in $\mathbf{Y}_{(t)}$ is more likely to be the same as that in the informative view with the largest scaling factor.

Theorem 3.5 indicates that $y_{ij(t)} \in \mathbf{Y}_{(t)}$ follows $y_{ij}^v \in \mathbf{Y}^v$ with a large scaling factor when different views have inconsistent clusters, which leverages the view with high confidence to correct other inconsistent views.

Theorem 3.6. (Complementarity & Noise robustness)

Case 1: if a sample representation is informative in some views and is noisy in other views, its cluster assignment in $\mathbf{Y}_{(t)}$ is the same as that in the informative views.

Case 2: if a sample representation is noisy in all views, its cluster assignment in $\mathbf{Y}_{(t)}$ is the same as the common cluster assignments existing in these views.

Theorem 3.6 illustrates the noise robustness of our method that makes the robust soft labels $\mathbf{Y}_{(t)}$ mitigate the side effects of noisy views. For example, $\mathbf{z}_i^v \in \mathbf{Z}^v$ is noisy in individual view but the corresponding scaled representation

$\mathbf{z}_{i(t)} \in \mathbf{Z}_{(t)}$ is informative, so the influence from noisy views on the soft labels $y_{ij(t)} \in \mathbf{Y}_{(t)}$ are reduced. Additionally, Theorems 3.5 and 3.6 can be together interpreted as the complementarity among multiple views, *i.e.*, the combination of multiple views is conducive to outperforming single views and discovering the comprehensive cluster patterns across multi-view data.

4. Experiments

4.1. Settings

Datasets. Four public datasets and their versions with extreme noise interference are used. Concretely, BDGP (Cai et al., 2012) is a drosophila embryos dataset where each sample contains a visual view and a textual view. DIGIT (Peng et al., 2019) is a dataset of handwritten arabic numbers in which each sample has two views coming from MNIST and USPS, respectively. COIL (Nene et al., 1996) is a multi-view dataset and the multiple views of one object are captured by the cameras from different visual angles. Amazon (Saenko et al., 2010) consists of the commodity images, such as bicycles, bags, and earphones. The raw samples are RGB images and we obtain the augmented data by rotation, horizontal flip, and color filter to construct the multi-view dataset. For each dataset, we randomly sample noise to build an additional view and obtain NoisyBDGP, NoisyDIGIT, NoisyCOIL, and NoisyAmazon, respectively.

Comparison methods. We compare MvCAN with 9 baselines including DEC, MVC-LFA, COMIC, DMJC, DIMC-net, EAMC, GP-MVC, DSMVC, and DSIMVC. The clustering effectiveness is evaluated by three widely used metrics, *i.e.*, clustering accuracy (ACC), normalized mutual information (NMI), and adjusted rand index (ARI). The average values of 10 runs are reported.

4.2. Comparison Results and Analysis

Table 1 reports all methods’ clustering effectiveness on four normal multi-view datasets, where DEC/BestV and DEC/WorstV denote the results of the single-view method (*i.e.*, DEC) on the best and the worst views, respectively. Firstly, based on the results of DEC/BestV and DEC/WorstV, it is easy to find the reality that the qualities of different views are different in normal multi-view datasets, where the views with unclear cluster structures could be considered as noisy views for some samples. Secondly, we find that the NVD adversely affect many MvC methods and these multi-view methods are not more robust than the single-view method in terms of clustering effectiveness. For example, although the multi-view methods (*e.g.*, MVC-LFA, COMIC, EAMC, and DSMVC) leverage multiple views’ information, they widely perform even worse than the single-view method DEC on some datasets (*e.g.*, BDGP and DIGIT).

These methods do not consider the NVD and the noisy views prevent them from learning effective cluster structures.

Instead, this work takes the NVD into account and theoretically investigates the multi-view consistency, complementarity, and noise robustness. The proposed MvCAN obtains much better performance than the single-view method and almost obtains the best performance among all multi-view methods. The improvements indicate that MvCAN can explore the useful consistent and complementary information among multiple views as well as achieve the robustness to noisy views.

Testing the noise robustness of the algorithms is helpful to understand their stability in practical scenarios. To this end, we conduct the experiments on multi-view datasets in the setting of extreme noise in Table 2. Compared with Table 1, the results in Table 2 indicate that most MvC methods have degenerated but our MvCAN still achieves the comparable performance. Specifically, MvCAN surpasses the best comparison methods by 3%, 9%, 1%, and 18% accuracy on the four noisy datasets, respectively. This further demonstrates the effectiveness of our method and theorems.

4.3. Ablation Study

Importance of two conditions in clustering objective. We investigate the importance of the two conditions in Eq. (5). As shown in Table 3, (i) Θ^v denotes the first condition of un-shared parameters for all views and (ii) \mathbf{A}^v indicates the second condition that every view is not required to be consistent. One could find that the results shown in (iii) achieve the best performance, which verifies the effectiveness of our MvCAN to mitigate the side effects caused by the NVD. Concretely, the un-shared $\{\Theta^v\}_{v=1}^V$ of all views eliminate their unfavourable interference. Moreover, $\{\mathbf{A}^v\}_{v=1}^V$ absolve the noisy views of conformity with the other views when minimizing the clustering objective.

Importance of two loss components in optimization. Table 4 lists the results of MvCAN with different loss components, where (a) denotes the clustering results of K -means on the direct concatenation of multi-view data. Compared with (a), both (b) and (c) can obtain improvements due to the representation learning objective achieved by \mathcal{L}_r and the clustering objective achieved by \mathcal{L}_c , respectively. (d) obtains the best performance which indicates that the representation learning objective and the clustering objective have the effect of mutual promotion in our MvCAN, verifying the importance of the two loss components.

Importance of bi-level optimization strategy. Figure 2 shows the performance by changing T_1 and T_2 in the first iteration of \mathcal{T} -level optimization and \mathcal{R} -level optimization. Based on the results, we have the observations as follows. When $T_1 = 1$ (*i.e.*, without \mathcal{T} -level optimization), MvCAN

Table 1. Comparison results on four normal datasets. Bold denotes the best results and underline denotes the second-best.

Datasets	BDGP			DIGIT			COIL			Amazon		
	ACC	NMI	ARI	ACC	NMI	ARI	ACC	NMI	ARI	ACC	NMI	ARI
DEC/BestV (Xie et al., 2016)	0.926	0.819	0.824	0.809	0.789	0.736	0.766	0.815	0.687	0.470	0.325	0.202
DEC/WorstV (Xie et al., 2016)	0.457	0.291	0.238	0.548	0.641	0.454	0.735	0.774	0.664	0.372	0.279	0.185
MVC-LFA (Wang et al., 2019)	0.547	0.335	0.288	0.768	0.675	0.609	0.860	0.868	0.799	0.440	0.514	0.414
COMIC (Peng et al., 2019)	0.578	0.642	0.427	0.482	0.709	0.510	0.796	0.916	0.729	0.386	0.327	0.215
DMJC (Xie et al., 2020)	0.678	0.465	0.412	0.976	0.962	0.950	0.913	0.938	0.876	0.633	0.653	0.480
DIMC-net (Wen et al., 2020)	0.975	0.911	0.927	0.904	0.873	0.896	0.985	0.975	0.961	0.625	<u>0.669</u>	<u>0.498</u>
EAMC (Zhou & Shen, 2020)	0.676	0.470	0.393	0.730	0.835	0.722	0.626	0.593	0.486	0.491	0.456	0.340
GP-MVC (Wang et al., 2021)	0.976	0.934	0.942	0.586	0.698	0.404	0.861	0.775	0.723	0.539	0.571	0.408
DSMVC (Tang & Liu, 2022a)	0.529	0.383	0.264	0.820	0.814	0.730	0.908	0.965	0.897	0.376	0.292	0.191
DSIMVC (Tang & Liu, 2022b)	0.980	0.940	0.951	0.990	0.971	0.977	0.997	0.990	0.989	0.646	0.578	0.484
MvCAN (The proposed)	0.984	0.953	0.961	0.995	0.988	0.989	0.996	0.991	0.990	0.826	0.867	0.779

Table 2. Comparison results on four datasets in the setting of extreme noise, where a noisy view is added to each dataset.

Datasets	NoisyBDGP			NoisyDIGIT			NoisyCOIL			NoisyAmazon		
	ACC	NMI	ARI	ACC	NMI	ARI	ACC	NMI	ARI	ACC	NMI	ARI
DEC/BestV (Xie et al., 2016)	0.926	0.819	0.824	0.809	0.789	0.736	0.766	0.815	0.687	0.470	0.325	0.202
DEC/WorstV (Xie et al., 2016)	0.222	0.002	0.000	0.124	0.004	0.000	0.164	0.028	0.002	0.120	0.004	0.000
MVC-LFA (Wang et al., 2019)	0.467	0.360	0.303	0.528	0.469	0.431	0.630	0.696	0.649	0.402	0.490	0.387
COMIC (Peng et al., 2019)	0.436	0.578	0.401	0.343	0.520	0.414	0.697	0.858	0.559	0.264	0.158	0.147
DMJC (Xie et al., 2020)	0.637	0.594	0.462	0.807	0.828	0.794	0.856	0.921	0.854	0.543	0.466	0.399
DIMC-net (Wen et al., 2020)	0.789	0.684	0.632	0.716	0.765	0.752	0.875	0.918	0.836	0.436	0.373	0.251
EAMC (Zhou & Shen, 2020)	0.625	0.396	0.345	0.308	0.473	0.433	0.636	0.364	0.349	0.407	0.360	0.242
GP-MVC (Wang et al., 2021)	0.807	0.784	0.796	0.491	0.635	0.395	0.694	0.729	0.673	0.404	0.398	0.229
DSMVC (Tang & Liu, 2022a)	0.571	0.418	0.316	0.737	0.722	0.629	0.818	0.841	0.750	0.366	0.259	0.166
DSIMVC (Tang & Liu, 2022b)	<u>0.951</u>	<u>0.852</u>	<u>0.883</u>	<u>0.904</u>	<u>0.905</u>	<u>0.870</u>	<u>0.988</u>	<u>0.978</u>	<u>0.975</u>	<u>0.547</u>	<u>0.541</u>	<u>0.429</u>
MvCAN (The proposed)	0.980	0.951	0.957	0.990	0.984	0.986	0.992	0.988	0.987	0.728	0.732	0.614

Table 3. Importance of two conditions in clustering objective.

	Conditions		BDGP			DIGIT			NoisyBDGP			NoisyDIGIT		
	Θ^v	\mathbf{A}^v	ACC	NMI	ARI	ACC	NMI	ARI	ACC	NMI	ARI	ACC	NMI	ARI
(i)	✓		0.973	0.921	0.935	0.986	0.980	0.982	0.977	0.946	0.949	0.902	0.933	0.884
(ii)		✓	0.660	0.477	0.451	0.840	0.735	0.690	0.602	0.339	0.305	0.611	0.599	0.436
(iii)	✓	✓	0.984	0.953	0.961	0.995	0.988	0.989	0.980	0.951	0.957	0.990	0.984	0.986

Table 4. Importance of two loss components in optimization.

	Components		BDGP			DIGIT			NoisyBDGP			NoisyDIGIT		
	\mathcal{L}_r	\mathcal{L}_c	ACC	NMI	ARI	ACC	NMI	ARI	ACC	NMI	ARI	ACC	NMI	ARI
(a)			0.643	0.522	0.245	0.768	0.723	0.635	0.499	0.315	0.253	0.741	0.705	0.611
(b)	✓		0.948	0.842	0.874	0.787	0.747	0.658	0.944	0.839	0.864	0.769	0.748	0.651
(c)		✓	0.798	0.709	0.656	0.870	0.943	0.867	0.726	0.574	0.381	0.591	0.702	0.504
(d)	✓	✓	0.984	0.953	0.961	0.995	0.988	0.989	0.980	0.951	0.957	0.990	0.984	0.986

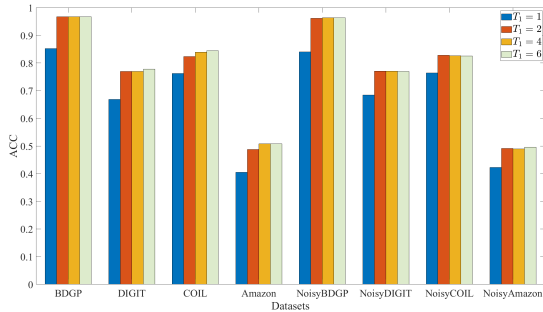
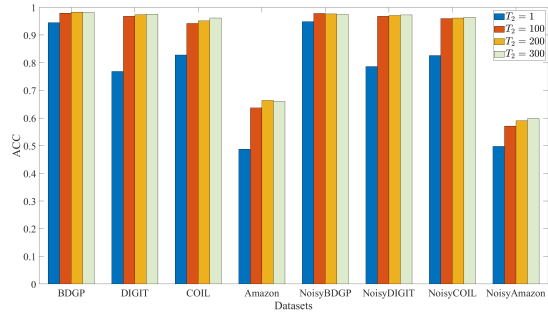

 (a) ACC vs. T_1 in \mathcal{T} -level optimization

 (b) ACC vs. T_2 in \mathcal{R} -level optimization

 Figure 2. Different training iterations in \mathcal{T} -level optimization and \mathcal{R} -level optimization of the proposed bi-level optimization strategy.

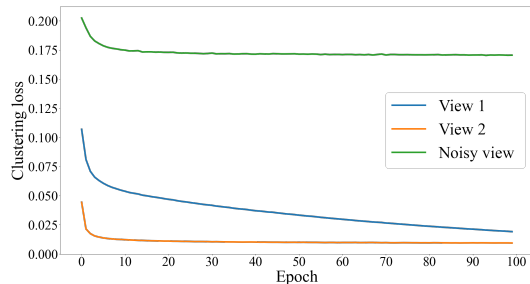


Figure 3. Loss vs. Epoch on NoisyBDGP.

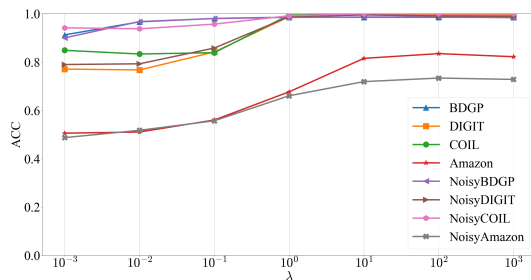
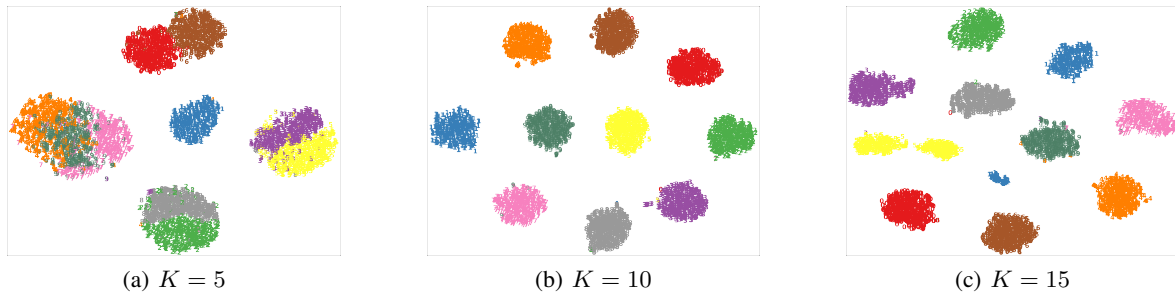

 Figure 4. ACC vs. λ .


Figure 5. Visualization of the representations learned with different prior knowledge of cluster numbers.

is unable to infer the effective scaling factors for different views to generate the robust learning target \mathbf{T} . Similarly, when $T_2 = 1$ (*i.e.*, without \mathcal{R} -level optimization), MvCAN cannot learn the effective representations with the learning target. When T_1 and T_2 increase, the performance also improves, which validates the effectiveness of our bi-level optimization strategy. Without loss of generality, we set $T_1 = 2$ and $T_2 = 100$ for all datasets tested in this paper.

4.4. Model Analysis

Convergence analysis. Figure 3 plots the clustering loss curve during training and we could observe that the model has good convergence properties. Moreover, it is worth noting that the loss values of the noisy views are larger than that of other views, which is consistent with our analysis in Section 2.2. Specifically, the features of the noisy view are not informative and have unclear cluster structures, which make the clustering objective difficult to be minimized. Therefore, we argue for using un-shared parameters and inconsistent clustering predictions for multiple views in the clustering objective of MvCAN, to alleviate the adverse impact of noisy views on the optimization process of other views.

Hyper-parameter analysis. The hyper-parameter of MvCAN includes the trade-off λ in Eq. (10) and Figure 4 shows the clustering effectiveness by traversing λ . The results indicate that λ is insensitive in the range of $[10^1, 10^3]$. Additionally, the cluster number K in the model is changeable. As shown in Figure 5, we utilize *t*-SNE (Maaten & Hinton, 2008) to visualize the scaled representations learned with different cluster numbers. For Dataset DIGIT, the truth K is

10. When K is small (*e.g.*, $K = 5$), we can observe that the representations of similar digits are closed, *e.g.*, “0” and “6” in Figure 5(a) (colored in red and brown). When K is large (*e.g.*, $K = 15$), we observe that the representations of the same digits are separated into two clusters, *e.g.*, “5” in Figure 5(c) (colored in yellow). Consequently, MvCAN could learn the coarse-grained or fine-grained cluster structures by changing the prior knowledge of K .

5. Conclusion and Discussion

This paper considered the pervasive but challenging problem in multi-view clustering, *i.e.*, Noisy-view Drawback (NVD). To alleviate the NVD, we proposed a novel deep multi-view clustering method, termed MvCAN. Comprehensive theoretical and empirical results verified the effectiveness of the two conditions in our proposed clustering objective, the non-parametric iterative process, and the bi-level optimization strategy. It might be promising to take the NVD into account, especially in unsupervised environments where the qualities of different views captured by various sensors cannot be guaranteed, *e.g.*, the views from some sensors are unreliable or not applicable and bring noisy information. Additionally, we find that the learned representations could be impacted by the prior knowledge of cluster numbers, hence our future work is to investigate the robustness on the number of cluster patterns in multi-view clustering.

References

- Abavisani, M. and Patel, V. M. Deep multimodal subspace clustering networks. *IEEE Journal of Selected Topics in Signal Processing*, 12(6):1601–1614, 2018.
- Bickel, S. and Scheffer, T. Multi-view clustering. In *ICDM*, pp. 19–26, 2004.
- Cai, X., Wang, H., Huang, H., and Ding, C. Joint stage recognition and anatomical annotation of drosophila gene expression patterns. *Bioinformatics*, 28(12):i16–i24, 2012.
- Cao, X., Zhang, C., Fu, H., Liu, S., and Zhang, H. Diversity-induced multi-view subspace clustering. In *CVPR*, pp. 586–594, 2015.
- Dalal, N. and Triggs, B. Histograms of oriented gradients for human detection. In *CVPR*, pp. 886–893, 2005.
- Du, G., Zhou, L., Lü, K., Wu, H., and Xu, Z. Multiview subspace clustering with multilevel representations and adversarial regularization. *IEEE Transactions on Neural Networks and Learning Systems*, 2022.
- Fan, S., Wang, X., Shi, C., Lu, E., Lin, K., and Wang, B. One2multi graph autoencoder for multi-view graph clustering. In *WWW*, pp. 3070–3076, 2020.
- Glorot, X., Bordes, A., and Bengio, Y. Deep sparse rectifier neural networks. In *AISTATS*, pp. 315–323, 2011.
- Goodfellow, I., Pouget-Abadie, J., Mirza, M., Xu, B., Warde-Farley, D., Ozair, S., Courville, A., and Bengio, Y. Generative adversarial nets. In *NeurIPS*, pp. 2672–2680, 2014.
- Guo, X., Gao, L., Liu, X., and Yin, J. Improved deep embedded clustering with local structure preservation. In *IJCAI*, pp. 1753–1759, 2017.
- Huang, Z., Hu, P., Zhou, J. T., Lv, J., and Peng, X. Partially view-aligned clustering. In *NeurIPS*, pp. 2892–2902, 2020.
- Kingma, D. P. and Ba, J. Adam: A method for stochastic optimization. In *ICLR*, 2015.
- Li, R., Zhang, C., Fu, H., Peng, X., Zhou, T., and Hu, Q. Reciprocal multi-layer subspace learning for multi-view clustering. In *ICCV*, pp. 8172–8180, 2019a.
- Li, Z., Wang, Q., Tao, Z., Gao, Q., and Yang, Z. Deep adversarial multi-view clustering network. In *IJCAI*, pp. 2952–2958, 2019b.
- Lin, Y., Gou, Y., Liu, Z., Li, B., Lv, J., and Peng, X. COMPLETE: Incomplete multi-view clustering via contrastive prediction. In *CVPR*, pp. 11174–11183, 2021.
- Liu, J., Wang, C., Gao, J., and Han, J. Multi-view clustering via joint nonnegative matrix factorization. In *SDM*, pp. 252–260, 2013.
- Liu, X., Zhu, X., Li, M., Wang, L., Tang, C., Yin, J., Shen, D., Wang, H., and Gao, W. Late fusion incomplete multi-view clustering. *IEEE Transactions on Pattern Analysis and Machine Intelligence*, 41(10):2410–2423, 2018.
- Liu, X., Liu, L., Liao, Q., Wang, S., Zhang, Y., Tu, W., Tang, C., Liu, J., and Zhu, E. One pass late fusion multi-view clustering. In *ICML*, pp. 6850–6859, 2021.
- Lowe, D. G. Distinctive image features from scale-invariant keypoints. *International Journal of Computer Vision*, 60(2):91–110, 2004.
- Maaten, L. v. d. and Hinton, G. Visualizing data using *t*-SNE. *Journal of Machine Learning Research*, 9:2579–2605, 2008.
- MacQueen, J. Some methods for classification and analysis of multivariate observations. In *BSMSP*, pp. 281–297, 1967.
- Nene, S. A., Nayar, S. K., Murase, H., et al. Columbia object image library (coil-100). <http://www1.cs.columbia.edu/CAVE/software/softlib/coil-100.php>, 1996.
- Ng, A. Y., Jordan, M. I., and Weiss, Y. On spectral clustering: Analysis and an algorithm. In *NeurIPS*, pp. 849–856, 2001.
- Nie, F., Li, J., and Li, X. Parameter-free auto-weighted multiple graph learning: a framework for multiview clustering and semi-supervised classification. In *IJCAI*, pp. 1881–1887, 2016.
- Nie, F., Tian, L., and Li, X. Multiview clustering via adaptively weighted procrustes. In *SIGKDD*, pp. 2022–2030, 2018.
- Ojala, T., Pietikainen, M., and Maenpaa, T. Multiresolution gray-scale and rotation invariant texture classification with local binary patterns. *IEEE Transactions on Pattern Analysis and Machine Intelligence*, 24(7):971–987, 2002.
- Pan, E. and Kang, Z. Multi-view contrastive graph clustering. In *NeurIPS*, pp. 2148–2159, 2021.
- Peng, X., Huang, Z., Lv, J., Zhu, H., and Zhou, J. T. COMIC: Multi-view clustering without parameter selection. In *ICML*, pp. 5092–5101, 2019.
- Saenko, K., Kulis, B., Fritz, M., and Darrell, T. Adapting visual category models to new domains. In *ECCV*, pp. 213–226, 2010.

- Tang, H. and Liu, Y. Deep safe multi-view clustering: Reducing the risk of clustering performance degradation caused by view increase. In *CVPR*, pp. 202–211, 2022a.
- Tang, H. and Liu, Y. Deep safe incomplete multi-view clustering: Theorem and algorithm. In *ICML*, pp. 21090–21110, 2022b.
- Tian, Y., Krishnan, D., and Isola, P. Contrastive multiview coding. In *ECCV*, pp. 776–794, 2020.
- Trosten, D. J., Løkse, S., Jenssen, R., and Kampffmeyer, M. Reconsidering representation alignment for multi-view clustering. In *CVPR*, pp. 1255–1265, 2021.
- Tzortzis, G. and Likas, A. Kernel-based weighted multi-view clustering. In *ICDM*, pp. 675–684, 2012.
- Wang, H., Nie, F., and Huang, H. Multi-view clustering and feature learning via structured sparsity. In *ICML*, pp. 352–360, 2013.
- Wang, Q., Ding, Z., Tao, Z., Gao, Q., and Fu, Y. Generative partial multi-view clustering with adaptive fusion and cycle consistency. *IEEE Transactions on Image Processing*, 30:1771–1783, 2021.
- Wang, S., Liu, X., Zhu, E., Tang, C., Liu, J., Hu, J., Xia, J., and Yin, J. Multi-view clustering via late fusion alignment maximization. In *IJCAI*, pp. 3778–3784, 2019.
- Wang, Y., Wenjie, Z., Wu, L., Lin, X., Fang, M., and Pan, S. Iterative views agreement: an iterative low-rank based structured optimization method to multi-view spectral clustering. In *IJCAI*, pp. 2153–2159, 2016.
- Wang, Y., Wu, L., Lin, X., and Gao, J. Multiview spectral clustering via structured low-rank matrix factorization. *IEEE Transactions on Neural Networks and Learning Systems*, 29(10):4833–4843, 2018.
- Wen, J., Xu, Y., and Liu, H. Incomplete multiview spectral clustering with adaptive graph learning. *IEEE Transactions on Cybernetics*, 50(4):1418–1429, 2018.
- Wen, J., Zhang, Z., Zhang, Z., Wu, Z., Fei, L., Xu, Y., and Zhang, B. DIMC-net: Deep incomplete multi-view clustering network. In *ACM MM*, pp. 3753–3761, 2020.
- Xie, J., Girshick, R., and Farhadi, A. Unsupervised deep embedding for clustering analysis. In *ICML*, pp. 478–487, 2016.
- Xie, Y., Lin, B., Qu, Y., Li, C., Zhang, W., Ma, L., Wen, Y., and Tao, D. Joint deep multi-view learning for image clustering. *IEEE Transactions on Knowledge and Data Engineering*, 33(11):3594–3606, 2020.
- Xu, C., Guan, Z., Zhao, W., Wu, H., Niu, Y., and Ling, B. Adversarial incomplete multi-view clustering. In *IJCAI*, pp. 3933–3939, 2019.
- Xu, J., Ren, Y., Tang, H., Pu, X., Zhu, X., Zeng, M., and He, L. Multi-VAE: Learning disentangled view-common and view-peculiar visual representations for multi-view clustering. In *ICCV*, pp. 9234–9243, 2021.
- Xu, J., Li, C., Ren, Y., Peng, L., Mo, Y., Shi, X., and Zhu, X. Deep incomplete multi-view clustering via mining cluster complementarity. In *AAAI*, pp. 8761–8769, 2022.
- Yang, M., Li, Y., Hu, P., Bai, J., Lv, J., and Peng, X. Robust multi-view clustering with incomplete information. *IEEE Transactions on Pattern Analysis and Machine Intelligence*, 45(1):1055–1069, 2022.
- Yang, Z., Liang, N., Yan, W., Li, Z., and Xie, S. Uniform distribution non-negative matrix factorization for multi-view clustering. *IEEE Transactions on Cybernetics*, pp. 3249–3262, 2021.
- Ye, Y., Liu, X., and Yin, J. Multi-view clustering with noisy views. In *CSAI*, pp. 339–344, 2018.
- Zhan, K., Nie, F., Wang, J., and Yang, Y. Multiview consensus graph clustering. *IEEE Transactions on Image Processing*, 28(3):1261–1270, 2018.
- Zhan, K., Niu, C., Chen, C., Nie, F., Zhang, C., and Yang, Y. Graph structure fusion for multiview clustering. *IEEE Transactions on Knowledge and Data Engineering*, 31(10):1984–1993, 2019.
- Zhang, C., Hu, Q., Fu, H., Zhu, P., and Cao, X. Latent multi-view subspace clustering. In *CVPR*, pp. 4279–4287, 2017.
- Zhang, C., Han, Z., Cui, Y., Fu, H., Zhou, J. T., and Hu, Q. CPM-Nets: Cross partial multi-view networks. In *NeurIPS*, pp. 557–567, 2019.
- Zhao, H., Ding, Z., and Fu, Y. Multi-view clustering via deep matrix factorization. In *AAAI*, pp. 2921–2927, 2017.
- Zhou, R. and Shen, Y.-D. End-to-end adversarial-attention network for multi-modal clustering. In *CVPR*, pp. 14619–14628, 2020.
- Zhou, T., Zhang, C., Peng, X., Bhaskar, H., and Yang, J. Dual shared-specific multiview subspace clustering. *IEEE Transactions on Cybernetics*, 50(8):3517–3530, 2019.

A. Related Work, Notations, and Our Framework

In the literature, existing multi-view clustering (MvC) methods could be divided into two groups, *i.e.*, traditional MvC methods and deep MvC methods.

Traditional MvC methods learn the representations of multi-view data for clustering by leveraging the classical machine learning technologies, such as graph MvC (Wen et al., 2018; Zhan et al., 2018; Peng et al., 2019; Pan & Kang, 2021), subspace MvC (Cao et al., 2015; Li et al., 2019a; Zhou et al., 2019), kernel MvC (Tzortzis & Likas, 2012; Liu et al., 2018; 2021), and matrix factorization MvC (Liu et al., 2013; Wang et al., 2018; Yang et al., 2021). However, traditional MvC methods are limited by their representation capability of shallow models such that they usually perform clustering only with the handcrafted features (Wang et al., 2013; 2016; Nie et al., 2016; Zhang et al., 2017), *e.g.*, local binary pattern (LBP (Ojala et al., 2002)), scale-invariant feature transform (SIFT (Lowe, 2004)), and histogram of oriented gradients (HOG (Dalal & Triggs, 2005)).

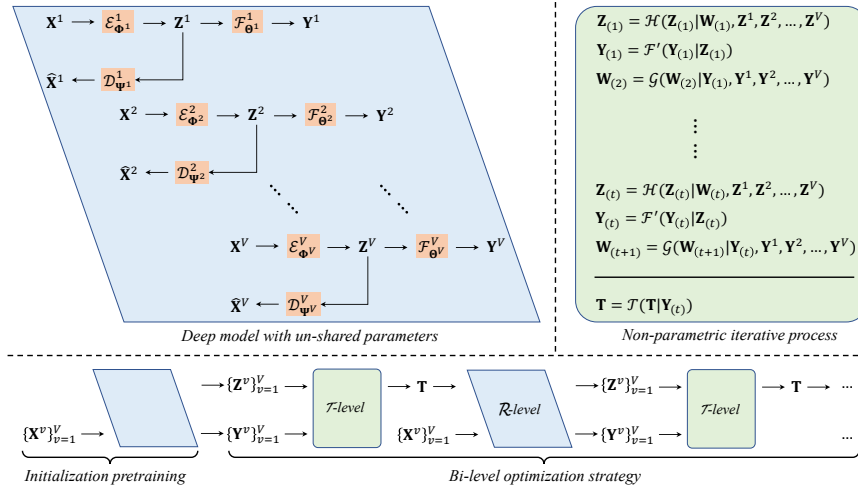


Figure 6. The framework of the proposed MvCAN.

During past years, many deep MvC methods have been proposed (Huang et al., 2020; Xu et al., 2021; Yang et al., 2022). Some deep MvC methods are based on the aforementioned machine learning technologies, such as deep subspace MvC (Abavisani & Patel, 2018; Du et al., 2022) and deep graph MvC (Fan et al., 2020; Pan & Kang, 2021). These deep MvC methods usually leverage the representation learning capability of deep neural networks as well as the data mining capability of traditional technologies. Besides, many works investigate various deep learning technologies to develop deep MvC methods. For example, some works (Xu et al., 2019; Li et al., 2019b; Zhou & Shen, 2020; Wang et al., 2021) combine the generative adversarial networks (GAN (Goodfellow et al., 2014)) with clustering objective for multiple views. Some works (Lin et al., 2021; Trosten et al., 2021; Pan & Kang, 2021) introduce the contrastive learning (Tian et al., 2020; Lin et al., 2021) to learn the consistency of multi-view representations for clustering. In research works, one of the most popular learning paradigms in deep MvC is based on the single-view clustering (SvC) method entitled deep embedded clustering (DEC (Xie et al., 2016)), *e.g.*, (Xu et al., 2019; Xie et al., 2020; Fan et al., 2020; Wen et al., 2020; Wang et al., 2021), which establishes a learning target to learn the clustering-oriented representations and are similar to self-supervised learning. Compared with traditional MvC methods, deep MvC methods have superior representation capability and thus they could handle clustering tasks on both raw features and handcrafted features.

However, in practical scenarios, previous works might ignore the noisy-view drawback (NVD) causing that MvC is not necessarily better than SvC, due to the fact that the features of samples extracted from some views could be noisy and might have no useful even harmful information for recognizing the samples. Although some efforts take the view quality into account and propose weighting strategies in the fusion of multiple views (Nie et al., 2018; Ye et al., 2018; Wen et al., 2020; Trosten et al., 2021; Wang et al., 2021), the low-quality views could be treated as a special case in the NVD and both the noisy views and the low-quality views will make it difficult to uncover the effective cluster patterns for most existing MvC methods (verified by Theorem B.1, Tables 1 and 2). There are two reasons that the NVD negatively affects the performance of existing MvC methods. First, previous works usually learn the representations by fusing multiple views, whereas the

Table 5. Notations and their descriptions in this paper.

Notations	Descriptions
N	the number of samples or the data size
V	the number of views in the multi-view dataset
K	the number of clusters in the multi-view dataset
i, j, k, v, t, e, m^*	the index notations
\mathbf{X}	the data for a single-view method, $\mathbf{x}_i \in \mathbf{X}$
\mathbf{Z}	the learned representation in a single-view method, $\mathbf{z}_i \in \mathbf{Z}$
\mathbf{Y}	the learned soft labels in a single-view method, $y_{ij} \in \mathbf{Y}$
\mathbf{T}	the learning target, $\mathbf{t}_i \in \mathbf{T}$, $t_{ij} \in \mathbf{T}$
\mathbf{X}^v	the v -th view's data for a multi-view method, $\mathbf{x}_i^v \in \mathbf{X}^v$
\mathbf{Z}^v	the learned representation of the v -th view in a multi-view method, $\mathbf{z}_i^v \in \mathbf{Z}^v$
\mathbf{Y}^v	the v -th view's soft labels in a multi-view method, $\mathbf{y}_i^v \in \mathbf{Y}^v$, $y_{ij}^v \in \mathbf{Y}^v$
$\hat{\mathbf{X}}^v$	the v -th view's reconstructed data for a multi-view method
D_v	the dimensionality of \mathbf{X}^v and $\hat{\mathbf{X}}^v$
d_v	the dimensionality of \mathbf{Z}^v
\mathcal{E}_Φ	the encoder with parameter Φ for a single-view method
μ_j	the j -th cluster centroid in a single-view method
\mathcal{E}_{Φ^v}	the v -th view's encoder with parameter Φ^v for a multi-view method
\mathcal{D}_{Ψ^v}	the v -th view's decoder with parameter Ψ^v for a multi-view method
μ_j^v	the j -th cluster centroid in the v -th view for a multi-view method
\mathcal{F}_Θ	the fusion module \mathcal{F} with the parameter Θ shared for multiple views
$\mathcal{F}_{\Theta^v}^v$	the v -th view's clustering module \mathcal{F}^v with the parameter Θ^v in MvCAN
$\mathcal{D}(\mathbf{a}, \mathbf{b})$	the squared Euclidean distance between representations \mathbf{a} and \mathbf{b}
$\mathcal{S}(\mathbf{a}, \mathbf{b})$	the similarity between representations \mathbf{a} and \mathbf{b}
ε	a sufficiently small value in Definitions
δ	a threshold in Theorems
\mathbf{L}	the ground-truth label matrix
\mathbf{A}	the matching matrix to calculate the clustering accuracy
$\tilde{\mathbf{Y}}$	the transformed prediction label matrix, $\tilde{\mathbf{y}}_i \in \tilde{\mathbf{Y}}$, $\tilde{y}_{ij} \in \tilde{\mathbf{Y}}$
\mathbf{A}^v	the matching matrix in the Condition 2 of MvCAN
$\mathbf{I}, \mathbf{I}_K, \mathbf{I}^v$	the unit matrices
$\mathbf{W}_{(t)}$	the scaling matrix in MvCAN, $w_{(t)}^v \in \mathbf{W}_{(t)}$
$\mathbf{Z}_{(t)}$	the scaled representation in MvCAN, $\mathbf{z}_{i(t)} \in \mathbf{Z}_{(t)}$
$\mathbf{Y}_{(t)}$	the robust soft labels in MvCAN, $y_{ij(t)} \in \mathbf{Y}_{(t)}$
$\mathbf{c}_{j(t)}$	the j -th cluster centroid of $\mathbf{Z}_{(t)}$ in the t -th iteration
\mathcal{L}_r	the representation learning objective of MvCAN
\mathcal{L}_c	the multi-view clustering objective of MvCAN
\mathcal{L}_K	the clustering objective of K -means
\mathcal{L}	the loss function to train the deep model in the \mathcal{R} -level optimization of MvCAN
λ	the hyper-parameter to achieve the trade-off between \mathcal{L}_r and \mathcal{L}_c
T_1	the iteration number in the \mathcal{T} -level optimization
T_2	the iteration number in the \mathcal{R} -level optimization
E	the number of training epoch
$\arg \max_j y_{ij}$	the cluster assignment for the i -th sample based on the soft label y_{ij}

parameters in the established fusion modules are shared by all views (Wang et al., 2016; Zhang et al., 2017; Zhou et al., 2019; Wang et al., 2019; Liu et al., 2021). Because the clustering objective punished on the noisy view might be dominant that on other informative views, causing the shared parameters to fit the noisy view and thus miss the useful information of other views. Second, many methods tend to obtain consistent clustering predictions for all views (Liu et al., 2013; Nie et al., 2016; Wang et al., 2018; Zhan et al., 2019; Zhou & Shen, 2020; Tang & Liu, 2022a; Xu et al., 2022). Nevertheless, it is

unreasonable to force the clustering prediction of the noisy view to be the same as that of other views, inversely, this process might make the learning and clustering on the informative views become worse.

To this end, we propose a novel deep MvC method, named MvCAN. The notations of this paper are listed in Table 5, and the framework of our proposed MvCAN is explained in Figure 6.

B. Proofs of Theorems

Theorem B.1. Denoting $\check{\mathbf{Y}} = \mathbf{L}\mathbf{A}$, where $\mathbf{A} \in \{0, 1\}^{K \times K}$ makes $\check{\mathbf{Y}}$ maximally match the learning target \mathbf{T} . Then, the clustering accuracy can be calculated as $ACC = \frac{1}{N} (N - \frac{1}{2} \|\check{\mathbf{Y}} - \mathbf{T}\|_F^2) = 1 - \frac{1}{2N} \|\check{\mathbf{Y}} - \mathbf{T}\|_F^2$. In Eq. (3), if Θ is shared by multiple views and their soft labels $\{\mathbf{Y}^v\}_{v=1}^V$ have consistent learning target \mathbf{T} , we have

$$ACC \leq 1 - \frac{1}{2N} \left(\left(\max_{1 \leq m \leq V} \|\check{\mathbf{Y}} - \mathcal{F}_\Theta(\mathbf{Y}^m | \{\mathbf{Z}^v\}_{v=1}^V)\|_F^2 \right) - \|\mathbf{T} - \mathcal{F}_\Theta(\mathbf{Y}^v | \{\mathbf{Z}^v\}_{v=1}^V)\|_F^2 \right). \quad (13)$$

Proof. Motivated by (Nie et al., 2018), we first consider the following equation:

$$\begin{aligned} & \|\check{\mathbf{Y}} - \mathcal{F}_\Theta(\mathbf{Y}^v | \{\mathbf{Z}^v\}_{v=1}^V)\|_F^2 - \|\mathbf{T} - \mathcal{F}_\Theta(\mathbf{Y}^v | \{\mathbf{Z}^v\}_{v=1}^V)\|_F^2 \\ &= \|\check{\mathbf{Y}}\|_F^2 - \|\mathbf{T}\|_F^2 + \|\mathcal{F}_\Theta(\mathbf{Y}^v | \{\mathbf{Z}^v\}_{v=1}^V)\|_F^2 - \|\mathcal{F}_\Theta(\mathbf{Y}^v | \{\mathbf{Z}^v\}_{v=1}^V)\|_F^2 - 2Tr \left((\check{\mathbf{Y}} - \mathbf{T})^T \mathcal{F}_\Theta(\mathbf{Y}^v | \{\mathbf{Z}^v\}_{v=1}^V) \right) \\ &= (N - \|\mathbf{T}\|_F^2) + (\|\mathcal{F}_\Theta(\mathbf{Y}^v | \{\mathbf{Z}^v\}_{v=1}^V)\|_F^2 - \|\mathcal{F}_\Theta(\mathbf{Y}^v | \{\mathbf{Z}^v\}_{v=1}^V)\|_F^2) - 2Tr \left((\check{\mathbf{Y}} - \mathbf{T})^T \mathcal{F}_\Theta(\mathbf{Y}^v | \{\mathbf{Z}^v\}_{v=1}^V) \right) \\ &= (N - \|\mathbf{T}\|_F^2) + 2Tr \left((\mathbf{T} - \check{\mathbf{Y}})^T \mathcal{F}_\Theta(\mathbf{Y}^v | \{\mathbf{Z}^v\}_{v=1}^V) \right) \\ &= (N - \|\mathbf{T}\|_F^2) + 2Tr \left(\mathcal{F}_\Theta(\mathbf{Y}^v | \{\mathbf{Z}^v\}_{v=1}^V) (\mathbf{T} - \check{\mathbf{Y}})^T \right), \end{aligned}$$

where the term of matrix trace could satisfy the inequality:

$$\begin{aligned} & 2Tr \left(\mathcal{F}_\Theta(\mathbf{Y}^v | \{\mathbf{Z}^v\}_{v=1}^V) (\mathbf{T} - \check{\mathbf{Y}})^T \right) \\ &= 2 \sum_{i=1}^N \mathbf{y}_i^v (\mathbf{t}_i^T - \check{\mathbf{y}}_i^T) \\ &= 2 \sum_{i=1}^N \mathbf{y}_i^v \mathbf{t}_i^T - \mathbf{y}_i^v \check{\mathbf{y}}_i^T \\ &= 2 \sum_{\mathbf{t}_i \neq \check{\mathbf{y}}_i} \left(\sum_{k=1}^K y_{ik}^v t_{ik} \right) - \left(\sum_{k=1}^K y_{ik}^v \check{y}_{ik} \right) \\ &\leq 2 \sum_{\mathbf{t}_i \neq \check{\mathbf{y}}_i} \left| \left(\sum_{k=1}^K y_{ik}^v t_{ik} \right) - \left(\sum_{k=1}^K y_{ik}^v \check{y}_{ik} \right) \right| \\ &\leq 2 \sum_{\mathbf{t}_i \neq \check{\mathbf{y}}_i} |1 - 0| \\ &= 2 \sum_{\mathbf{t}_i \neq \check{\mathbf{y}}_i} 1 \\ &= \|\check{\mathbf{Y}} - \mathbf{T}\|_F^2. \end{aligned}$$

Then, we have

$$\begin{aligned} \|\check{\mathbf{Y}} - \mathbf{T}\|_F^2 &\geq \|\check{\mathbf{Y}} - \mathcal{F}_\Theta(\mathbf{Y}^v | \{\mathbf{Z}^v\}_{v=1}^V)\|_F^2 - \|\mathbf{T} - \mathcal{F}_\Theta(\mathbf{Y}^v | \{\mathbf{Z}^v\}_{v=1}^V)\|_F^2 - N + \|\mathbf{T}\|_F^2 \\ &\geq \left(\max_{1 \leq m \leq V} \|\check{\mathbf{Y}} - \mathcal{F}_\Theta(\mathbf{Y}^m | \{\mathbf{Z}^v\}_{v=1}^V)\|_F^2 \right) - \|\mathbf{T} - \mathcal{F}_\Theta(\mathbf{Y}^v | \{\mathbf{Z}^v\}_{v=1}^V)\|_F^2 - N + \left(\max_{\mathbf{T}} \|\mathbf{T}\|_F^2 \right) \\ &\geq \left(\max_{1 \leq m \leq V} \|\check{\mathbf{Y}} - \mathcal{F}_\Theta(\mathbf{Y}^m | \{\mathbf{Z}^v\}_{v=1}^V)\|_F^2 \right) - \|\mathbf{T} - \mathcal{F}_\Theta(\mathbf{Y}^v | \{\mathbf{Z}^v\}_{v=1}^V)\|_F^2. \end{aligned}$$

Furthermore, the clustering accuracy becomes

$$\begin{aligned} ACC &= \frac{1}{N} \left(N - \frac{1}{2} \|\tilde{\mathbf{Y}} - \mathbf{T}\|_F^2 \right) = 1 - \frac{1}{2N} \|\tilde{\mathbf{Y}} - \mathbf{T}\|_F^2 \\ &\leq 1 - \frac{1}{2N} \left(\left(\max_{1 \leq m \leq V} \|\tilde{\mathbf{Y}} - \mathcal{F}_{\Theta}(\mathbf{Y}^m | \{\mathbf{Z}^v\}_{v=1}^V)\|_F^2 \right) - \|\mathbf{T} - \mathcal{F}_{\Theta}(\mathbf{Y}^v | \{\mathbf{Z}^v\}_{v=1}^V)\|_F^2 \right), \end{aligned}$$

which completes this proof. \square

A specific example for illustrating Theorem B.1. Given the DEC framework as a specific example, we denote \mathbf{Z}^m and \mathbf{Z}^n , respectively, as the representations of the informative view and the noisy/low-quality view. The shared parameters are the K cluster centroids $\mathbf{U} = [\boldsymbol{\mu}_1, \boldsymbol{\mu}_2, \dots, \boldsymbol{\mu}_K]$, which are shared for all views' representations. Based on \mathbf{Z}^m and \mathbf{U} as formulated in Eq. (1), the informative view's representation \mathbf{Z}^m has clear cluster structures and thus its clustering loss \mathcal{L}_c^m is easy to minimize. However, based on \mathbf{Z}^n and the same \mathbf{U} as formulated in Eq. (1), the noisy/low-quality view's representation \mathbf{Z}^n has unclear cluster structures and thus its clustering loss \mathcal{L}_c^n is hard to minimize. On the one hand, since the training objectives of multiple views have the same learning target \mathbf{T} , the large \mathcal{L}_c^n will dominate the small \mathcal{L}_c^m if their optimizations are not decoupled. On the other hand, the minimization of the noisy view's clustering loss \mathcal{L}_c^n will change the shared K cluster centroids \mathbf{U} , causing that \mathbf{U} is not suitable for the informative view's representations \mathbf{Z}^m . As a result, the NVD of low-quality or noisy views destroys the methods' robustness.

Theorem B.2. Denoting \mathcal{L}_K as the K -means objective, $\mathcal{L}_K(\mathbf{Z}_{(t)})$ is equivalent to punishing different scaling factors on $\{\mathcal{L}_K(\mathbf{Z}^v)\}_{v=1}^V$ under the consistency constraint of multiple views' cluster centroids.

Proof. For clarity, we may omit the iteration symbol (t) of $\mathbf{Z}_{(t)}$, $\mathbf{W}_{(t)}$, and $\mathbf{c}_{j(t)}$ in next proofs. Then, the K -means objective on \mathbf{Z} (i.e., $\mathbf{Z}_{(t)}$) can be formulated as:

$$\begin{aligned} \mathcal{L}_K(\mathbf{Z}) &= \min_{\mathbf{c}_j} \sum_{i=1}^N \sum_{j=1}^K \|\mathbf{z}_i - \mathbf{c}_j\|_2^2 \\ &= \min_{\boldsymbol{\mu}_j^v} \sum_{i=1}^N \sum_{j=1}^K \sum_{v=1}^V \|w^v \mathbf{z}_i^v - w^v \boldsymbol{\mu}_j^v\|_2^2, \text{ s.t. } \mathbf{c}_j = [\boldsymbol{\mu}_j^1 \quad \boldsymbol{\mu}_j^2 \quad \dots \quad \boldsymbol{\mu}_j^V] \mathbf{W} \\ &= \sum_{v=1}^V (w^v)^2 \min_{\boldsymbol{\mu}_j^v} \sum_{i=1}^N \sum_{j=1}^K \|\mathbf{z}_i^v - \boldsymbol{\mu}_j^v\|_2^2, \text{ s.t. } \mathbf{c}_j = [\boldsymbol{\mu}_j^1 \quad \boldsymbol{\mu}_j^2 \quad \dots \quad \boldsymbol{\mu}_j^V] \mathbf{W} \\ &= \sum_{v=1}^V (w^v)^2 \mathcal{L}_K(\mathbf{Z}^v), \text{ s.t. } \mathbf{c}_j = [\boldsymbol{\mu}_j^1 \quad \boldsymbol{\mu}_j^2 \quad \dots \quad \boldsymbol{\mu}_j^V] \mathbf{W}, \end{aligned}$$

where \mathbf{c}_j and $\boldsymbol{\mu}_j^v$ denote the j -th cluster centroid of \mathbf{Z} and \mathbf{Z}^v , respectively. First, we can find that $(w^v)^2 \mathcal{L}_K(\mathbf{Z}^v)$ punishes different scaling factors on different views. Second, if the K -means objective is conducted on \mathbf{Z}^v individually, the obtained cluster centroids for the same cluster of two views might have different samples, e.g., $\boldsymbol{\mu}_j^a = 1/\sum_{i \in \Omega^a} \mathbf{z}_i^a$ and $\boldsymbol{\mu}_j^b = 1/\sum_{i \in \Omega^b} \mathbf{z}_i^b$ where $\Omega^a \neq \Omega^b$. However, the constraint condition $\mathbf{c}_j = [\boldsymbol{\mu}_j^1 \quad \boldsymbol{\mu}_j^2 \quad \dots \quad \boldsymbol{\mu}_j^V] \mathbf{W}$ makes $\Omega^a = \Omega^b = \Omega^c$ such that $w^a \boldsymbol{\mu}_j^a = 1/\sum_{i \in \Omega^a} w^a \mathbf{z}_i^a$, $w^b \boldsymbol{\mu}_j^b = 1/\sum_{i \in \Omega^b} w^b \mathbf{z}_i^b$, and $\mathbf{c}_j = 1/\sum_{i \in \Omega^c} \mathbf{z}_i$ for $\forall a, b \in \{1, 2, \dots, V\}$. Therefore, the constraint condition could be treated as the consistency constraint of multiple views' cluster centroids, which guarantees that $\mathbf{c}_j, \boldsymbol{\mu}_j^1, \boldsymbol{\mu}_j^2, \dots, \boldsymbol{\mu}_j^V$ represent the centroids for the same cluster. \square

Theorem B.3. (Consistency) If a sample representation is informative in multiple views and has the same cluster assignments in these views, its cluster assignment in $\mathbf{Y}_{(t)}$ is the same as that in these views.

Proof. For clarity, we take two views as example, $\mathbf{z}_i = [w^1 \mathbf{z}_i^1 \quad w^2 \mathbf{z}_i^2] \in \mathbf{Z}$ and we let $\mathbf{c}_j = [w^1 \boldsymbol{\mu}_j^1 \quad w^2 \boldsymbol{\mu}_j^2]$ denote the ideal cluster centroid in the scaled representation space of \mathbf{Z} , where $\boldsymbol{\mu}_j^1$ and $\boldsymbol{\mu}_j^2$ are the cluster centroids in the 1-st view and

the 2-nd view of the j -th cluster, respectively. For any two clusters, *e.g.*, \mathbf{c}_1 and \mathbf{c}_2 , we have

$$\begin{aligned} \mathcal{D}(\mathbf{z}_i, \mathbf{c}_1) &= \left\| [w^1 \mathbf{z}_i^1 \quad w^2 \mathbf{z}_i^2] - [w^1 \boldsymbol{\mu}_1^1 \quad w^2 \boldsymbol{\mu}_1^2] \right\|_2^2 \\ &= \left\| w^1 \mathbf{z}_i^1 - w^1 \boldsymbol{\mu}_1^1 \right\|_2^2 + \left\| w^2 \mathbf{z}_i^2 - w^2 \boldsymbol{\mu}_1^2 \right\|_2^2 \\ &= (w^1)^2 \left\| \mathbf{z}_i^1 - \boldsymbol{\mu}_1^1 \right\|_2^2 + (w^2)^2 \left\| \mathbf{z}_i^2 - \boldsymbol{\mu}_1^2 \right\|_2^2 \\ &= (w^1)^2 \mathcal{D}(\mathbf{z}_i^1, \boldsymbol{\mu}_1^1) + (w^2)^2 \mathcal{D}(\mathbf{z}_i^2, \boldsymbol{\mu}_1^2). \end{aligned}$$

Similarly, $\mathcal{D}(\mathbf{z}_i, \mathbf{c}_2) = (w^1)^2 \mathcal{D}(\mathbf{z}_i^1, \boldsymbol{\mu}_2^1) + (w^2)^2 \mathcal{D}(\mathbf{z}_i^2, \boldsymbol{\mu}_2^2)$. Furthermore, we have

$$\begin{aligned} \mathcal{D}(\mathbf{z}_i, \mathbf{c}_1) - \mathcal{D}(\mathbf{z}_i, \mathbf{c}_2) &= (w^1)^2 \mathcal{D}(\mathbf{z}_i^1, \boldsymbol{\mu}_1^1) + (w^2)^2 \mathcal{D}(\mathbf{z}_i^2, \boldsymbol{\mu}_1^2) - (w^1)^2 \mathcal{D}(\mathbf{z}_i^1, \boldsymbol{\mu}_2^1) - (w^2)^2 \mathcal{D}(\mathbf{z}_i^2, \boldsymbol{\mu}_2^2) \\ &= (w^1)^2 (\mathcal{D}(\mathbf{z}_i^1, \boldsymbol{\mu}_1^1) - \mathcal{D}(\mathbf{z}_i^1, \boldsymbol{\mu}_2^1)) + (w^2)^2 (\mathcal{D}(\mathbf{z}_i^2, \boldsymbol{\mu}_1^2) - \mathcal{D}(\mathbf{z}_i^2, \boldsymbol{\mu}_2^2)). \end{aligned}$$

If $y_{i1}^1 > y_{i2}^1$ and $y_{i1}^2 > y_{i2}^2$, the sample is informative in both views and has the same cluster assignment, *i.e.*, $\mathcal{D}(\mathbf{z}_i^1, \boldsymbol{\mu}_1^1) < \mathcal{D}(\mathbf{z}_i^1, \boldsymbol{\mu}_2^1)$ and $\mathcal{D}(\mathbf{z}_i^2, \boldsymbol{\mu}_1^2) < \mathcal{D}(\mathbf{z}_i^2, \boldsymbol{\mu}_2^2)$. Then, the following inequality holds:

$$\mathcal{D}(\mathbf{z}_i, \mathbf{c}_1) - \mathcal{D}(\mathbf{z}_i, \mathbf{c}_2) = (w^1)^2 (\mathcal{D}(\mathbf{z}_i^1, \boldsymbol{\mu}_1^1) - \mathcal{D}(\mathbf{z}_i^1, \boldsymbol{\mu}_2^1)) + (w^2)^2 (\mathcal{D}(\mathbf{z}_i^2, \boldsymbol{\mu}_1^2) - \mathcal{D}(\mathbf{z}_i^2, \boldsymbol{\mu}_2^2)) < 0,$$

which indicates that $y_{i1} > y_{i2}$. Similarly, if $y_{i1}^1 < y_{i2}^1$ and $y_{i1}^2 < y_{i2}^2$, we have $\mathcal{D}(\mathbf{z}_i^1, \boldsymbol{\mu}_1^1) > \mathcal{D}(\mathbf{z}_i^1, \boldsymbol{\mu}_2^1)$, $\mathcal{D}(\mathbf{z}_i^2, \boldsymbol{\mu}_1^2) > \mathcal{D}(\mathbf{z}_i^2, \boldsymbol{\mu}_2^2)$, and $\mathcal{D}(\mathbf{z}_i, \mathbf{c}_1) - \mathcal{D}(\mathbf{z}_i, \mathbf{c}_2) > 0$ which indicates that $y_{i1} < y_{i2}$. As a result, the sample has the same cluster assignment in $\mathbf{Y}_{(t)}$ as that in the informative views, *i.e.*, \mathbf{Y}^1 and \mathbf{Y}^2 . \square

Theorem B.4. (Complementarity) *If a sample representation is informative in multiple views where it has different cluster assignments, we have two cases according to the differences of similarity among the clusters.*

Case 1: if the differences of similarity among the clusters are equal, its cluster assignment in $\mathbf{Y}_{(t)}$ is the same as that in the informative view with the largest scaling factor.

Case 2: if the differences of similarity among the clusters are not equal, its cluster assignment in $\mathbf{Y}_{(t)}$ is more likely to be the same as that in the informative view with the largest scaling factor.

Proof. Letting $\Delta^v = |\mathcal{D}(\mathbf{z}_i^v, \boldsymbol{\mu}_1^v) - \mathcal{D}(\mathbf{z}_i^v, \boldsymbol{\mu}_2^v)|$, and $\Gamma^v = |\mathcal{S}(\mathbf{z}_i^v, \boldsymbol{\mu}_1^v) - \mathcal{S}(\mathbf{z}_i^v, \boldsymbol{\mu}_2^v)|$ denote the difference of similarity, we have $\Delta^1 = \Delta^2 \Rightarrow |\mathcal{S}(\mathbf{z}_i^1, \boldsymbol{\mu}_1^1) - \mathcal{S}(\mathbf{z}_i^1, \boldsymbol{\mu}_2^1)| = |\mathcal{S}(\mathbf{z}_i^2, \boldsymbol{\mu}_1^2) - \mathcal{S}(\mathbf{z}_i^2, \boldsymbol{\mu}_2^2)|$.

Case 1: if $(\mathcal{D}(\mathbf{z}_i^1, \boldsymbol{\mu}_1^1) - \mathcal{D}(\mathbf{z}_i^1, \boldsymbol{\mu}_2^1))(\mathcal{D}(\mathbf{z}_i^2, \boldsymbol{\mu}_1^2) - \mathcal{D}(\mathbf{z}_i^2, \boldsymbol{\mu}_2^2)) < 0$ and $\Delta^1 = \Delta^2$, the sample is informative in both views but it has different cluster assignments (*i.e.*, $\arg \max_j y_{ij}^1 \neq \arg \max_j y_{ij}^2$), and the differences of similarity are equal $\Gamma^1 = \Gamma^2$. In this case, we obtain a boundary condition:

$$\mathcal{D}(\mathbf{z}_i^1, \boldsymbol{\mu}_1^1) - \mathcal{D}(\mathbf{z}_i^1, \boldsymbol{\mu}_2^1) = \mathcal{D}(\mathbf{z}_i^2, \boldsymbol{\mu}_2^2) - \mathcal{D}(\mathbf{z}_i^2, \boldsymbol{\mu}_1^2),$$

and thus $\mathcal{D}(\mathbf{z}_i, \mathbf{c}_1) - \mathcal{D}(\mathbf{z}_i, \mathbf{c}_2)$ in Theorem B.3 becomes

$$\begin{aligned} \mathcal{D}(\mathbf{z}_i, \mathbf{c}_1) - \mathcal{D}(\mathbf{z}_i, \mathbf{c}_2) &= (w^1)^2 (\mathcal{D}(\mathbf{z}_i^1, \boldsymbol{\mu}_1^1) - \mathcal{D}(\mathbf{z}_i^1, \boldsymbol{\mu}_2^1)) + (w^2)^2 (\mathcal{D}(\mathbf{z}_i^2, \boldsymbol{\mu}_1^2) - \mathcal{D}(\mathbf{z}_i^2, \boldsymbol{\mu}_2^2)) \\ &= ((w^1)^2 - (w^2)^2) (\mathcal{D}(\mathbf{z}_i^1, \boldsymbol{\mu}_1^1) - \mathcal{D}(\mathbf{z}_i^1, \boldsymbol{\mu}_2^1)). \end{aligned}$$

If $w^1 > w^2$, we further have

$$\begin{aligned} y_{i1}^1 > y_{i2}^1 &\Rightarrow \mathcal{D}(\mathbf{z}_i^1, \boldsymbol{\mu}_1^1) < \mathcal{D}(\mathbf{z}_i^1, \boldsymbol{\mu}_2^1) \\ &\Rightarrow \mathcal{D}(\mathbf{z}_i, \mathbf{c}_1) < \mathcal{D}(\mathbf{z}_i, \mathbf{c}_2) \\ &\Rightarrow y_{i1} > y_{i2} \end{aligned}$$

and $y_{i1}^1 < y_{i2}^1 \Rightarrow y_{i1} < y_{i2}$.

If $w^1 < w^2$, we similarly have

$$\begin{aligned} y_{i1}^2 > y_{i2}^2 &\Rightarrow \mathcal{D}(\mathbf{z}_i^2, \boldsymbol{\mu}_1^2) < \mathcal{D}(\mathbf{z}_i^2, \boldsymbol{\mu}_2^2) \\ &\Rightarrow \mathcal{D}(\mathbf{z}_i^1, \boldsymbol{\mu}_1^1) > \mathcal{D}(\mathbf{z}_i^1, \boldsymbol{\mu}_2^1) \\ &\Rightarrow \mathcal{D}(\mathbf{z}_i, \mathbf{c}_1) < \mathcal{D}(\mathbf{z}_i, \mathbf{c}_2) \\ &\Rightarrow y_{i1} > y_{i2} \end{aligned}$$

and $y_{i1}^2 < y_{i2}^2 \Rightarrow y_{i1} < y_{i2}$. \Rightarrow' holds because $(\mathcal{D}(\mathbf{z}_i^1, \mu_1^1) - \mathcal{D}(\mathbf{z}_i^1, \mu_2^1))(\mathcal{D}(\mathbf{z}_i^2, \mu_1^2) - \mathcal{D}(\mathbf{z}_i^2, \mu_2^2)) < 0$. In conclusion, the sample has the same cluster assignment in $\mathbf{Y}_{(t)}$ as that the view with the largest scaling factor.

Case 2: if $(\mathcal{D}(\mathbf{z}_i^1, \mu_1^1) - \mathcal{D}(\mathbf{z}_i^1, \mu_2^1))(\mathcal{D}(\mathbf{z}_i^2, \mu_1^2) - \mathcal{D}(\mathbf{z}_i^2, \mu_2^2)) < 0$ and $\Delta^1 \neq \Delta^2$, the sample is informative in both views but it has different cluster assignments (*i.e.*, $\arg \max_j y_{ij}^1 \neq \arg \max_j y_{ij}^2$), and the differences of similarity are not equal $\Gamma^1 \neq \Gamma^2$.

In this case, if $y_{i1}^1 < y_{i2}^1$ and $y_{i1}^2 > y_{i2}^2$, *i.e.*, $\mathcal{D}(\mathbf{z}_i^1, \mu_1^1) > \mathcal{D}(\mathbf{z}_i^1, \mu_2^1)$ and $\mathcal{D}(\mathbf{z}_i^2, \mu_1^2) < \mathcal{D}(\mathbf{z}_i^2, \mu_2^2)$, there is a threshold δ as $\mathcal{D}(\mathbf{z}_i^1, \mu_1^1) \neq \mathcal{D}(\mathbf{z}_i^1, \mu_2^1)$ and $\mathcal{D}(\mathbf{z}_i^2, \mu_1^2) \neq \mathcal{D}(\mathbf{z}_i^2, \mu_2^2)$:

$$\delta = \frac{\Delta^2}{\Delta^1} = \frac{\mathcal{D}(\mathbf{z}_i^2, \mu_2^2) - \mathcal{D}(\mathbf{z}_i^2, \mu_1^2)}{\mathcal{D}(\mathbf{z}_i^1, \mu_1^1) - \mathcal{D}(\mathbf{z}_i^1, \mu_2^1)}.$$

When w^1 is large so that $\frac{(w^1)^2}{(w^2)^2} > \delta$, we have

$$\begin{aligned} \frac{(w^1)^2}{(w^2)^2} &> \frac{\mathcal{D}(\mathbf{z}_i^2, \mu_2^2) - \mathcal{D}(\mathbf{z}_i^2, \mu_1^2)}{\mathcal{D}(\mathbf{z}_i^1, \mu_1^1) - \mathcal{D}(\mathbf{z}_i^1, \mu_2^1)} \\ \Rightarrow (w^1)^2 (\mathcal{D}(\mathbf{z}_i^1, \mu_1^1) - \mathcal{D}(\mathbf{z}_i^1, \mu_2^1)) &+ (w^2)^2 (\mathcal{D}(\mathbf{z}_i^2, \mu_1^2) - \mathcal{D}(\mathbf{z}_i^2, \mu_2^2)) > 0 \\ \Rightarrow \mathcal{D}(\mathbf{z}_i, \mathbf{c}_1) - \mathcal{D}(\mathbf{z}_i, \mathbf{c}_2) &> 0 \\ \Rightarrow y_{i1} < y_{i2}, \end{aligned}$$

which indicates $y_{i1}^1 < y_{i2}^1 \Rightarrow y_{i1} < y_{i2}$, *i.e.*, the sample has the same cluster assignment in $\mathbf{Y}_{(t)}$ as that in the view with the scaling factor w^1 .

When w^2 is large so that $\frac{(w^1)^2}{(w^2)^2} < \delta$, we have

$$\begin{aligned} \frac{(w^1)^2}{(w^2)^2} &< \frac{\mathcal{D}(\mathbf{z}_i^2, \mu_2^2) - \mathcal{D}(\mathbf{z}_i^2, \mu_1^2)}{\mathcal{D}(\mathbf{z}_i^1, \mu_1^1) - \mathcal{D}(\mathbf{z}_i^1, \mu_2^1)} \\ \Rightarrow (w^1)^2 (\mathcal{D}(\mathbf{z}_i^1, \mu_1^1) - \mathcal{D}(\mathbf{z}_i^1, \mu_2^1)) &+ (w^2)^2 (\mathcal{D}(\mathbf{z}_i^2, \mu_1^2) - \mathcal{D}(\mathbf{z}_i^2, \mu_2^2)) < 0 \\ \Rightarrow \mathcal{D}(\mathbf{z}_i, \mathbf{c}_1) - \mathcal{D}(\mathbf{z}_i, \mathbf{c}_2) &< 0 \\ \Rightarrow y_{i1} > y_{i2}, \end{aligned}$$

which indicates $y_{i1}^2 > y_{i2}^2 \Rightarrow y_{i1} > y_{i2}$, *i.e.*, the sample has the same cluster assignment in $\mathbf{Y}_{(t)}$ as that in the view with the scaling factor w^2 .

Similarly, if $y_{i1}^1 > y_{i2}^1$ and $y_{i1}^2 < y_{i2}^2$, *i.e.*, $\mathcal{D}(\mathbf{z}_i^1, \mu_1^1) < \mathcal{D}(\mathbf{z}_i^1, \mu_2^1)$ and $\mathcal{D}(\mathbf{z}_i^2, \mu_1^2) > \mathcal{D}(\mathbf{z}_i^2, \mu_2^2)$, we have the same conclusions. Therefore, if we put a large scaling factor on the v -th view, the sample is more likely to have the same cluster assignment as that in the v -th view. \square

Theorem B.5. (Complementarity & Noise robustness)

Case 1: if a sample representation is informative in some views and is noisy in other views, its cluster assignment in $\mathbf{Y}_{(t)}$ is the same as that in the informative views.

Case 2: if a sample representation is noisy in all views, its cluster assignment in $\mathbf{Y}_{(t)}$ is the same as the common cluster assignments existing in these views.

Proof. Case 1: if a sample is informative in some views and is noisy in other views, we can treat all noisy views as one noisy view and all informative views as one informative view, *e.g.*, $\mathbf{z}_i^1 = [w^a \mathbf{z}_i^a \quad w^b \mathbf{z}_i^b]$ denotes the noisy view and $\mathbf{z}_i^2 = [w^c \mathbf{z}_i^c \quad w^d \mathbf{z}_i^d]$ denotes the informative view, where \mathbf{z}_i^a and \mathbf{z}_i^b are noisy while \mathbf{z}_i^c and \mathbf{z}_i^d are informative. Let $w^v = 1$ in Theorem B.3, $\mathcal{D}(\mathbf{z}_i, \mathbf{c}_1) - \mathcal{D}(\mathbf{z}_i, \mathbf{c}_2)$ becomes

$$\begin{aligned} \mathcal{D}(\mathbf{z}_i, \mathbf{c}_1) - \mathcal{D}(\mathbf{z}_i, \mathbf{c}_2) &= \mathcal{D}(\mathbf{z}_i^1, \mu_1^1) + \mathcal{D}(\mathbf{z}_i^2, \mu_1^2) - \mathcal{D}(\mathbf{z}_i^1, \mu_2^1) - \mathcal{D}(\mathbf{z}_i^2, \mu_2^2) \\ &= (\mathcal{D}(\mathbf{z}_i^1, \mu_1^1) - \mathcal{D}(\mathbf{z}_i^1, \mu_2^1)) + (\mathcal{D}(\mathbf{z}_i^2, \mu_1^2) - \mathcal{D}(\mathbf{z}_i^2, \mu_2^2)). \end{aligned}$$

If $|\mathcal{D}(\mathbf{z}_i^1, \mu_1^1) - \mathcal{D}(\mathbf{z}_i^1, \mu_2^1)| < \varepsilon$ and $\mathcal{D}(\mathbf{z}_i^2, \mu_1^2) \neq \mathcal{D}(\mathbf{z}_i^2, \mu_2^2)$, *i.e.*, the sample is noisy in the 1-st view but informative in the 2-nd view. As ε is a sufficiently small value, we have

$$\mathcal{D}(\mathbf{z}_i, \mathbf{c}_1) - \mathcal{D}(\mathbf{z}_i, \mathbf{c}_2) \approx \mathcal{D}(\mathbf{z}_i^2, \mu_1^2) - \mathcal{D}(\mathbf{z}_i^2, \mu_2^2).$$

According to the definitions, we obtain the conclusion:

$$\begin{aligned}
 y_{i1}^2 > y_{i2}^2 &\Rightarrow \mathcal{D}(\mathbf{z}_i^2, \boldsymbol{\mu}_1^2) < \mathcal{D}(\mathbf{z}_i^2, \boldsymbol{\mu}_2^2) \\
 &\Rightarrow \mathcal{D}(\mathbf{z}_i, \mathbf{c}_1) < \mathcal{D}(\mathbf{z}_i, \mathbf{c}_2) \\
 &\Rightarrow \mathcal{S}(\mathbf{z}_i, \mathbf{c}_1) > \mathcal{S}(\mathbf{z}_i, \mathbf{c}_2) \\
 &\Rightarrow y_{i1} > y_{i2}
 \end{aligned}$$

and $y_{i1}^2 < y_{i2}^2 \Rightarrow y_{i1} < y_{i2}$, which indicates that the sample has the same cluster assignment in $\mathbf{Y}_{(t)}$ as that in \mathbf{Y}^2 of the informative views. Similarly, if $\mathcal{D}(\mathbf{z}_i^1, \boldsymbol{\mu}_1^1) \neq \mathcal{D}(\mathbf{z}_i^1, \boldsymbol{\mu}_2^1)$ and $|\mathcal{D}(\mathbf{z}_i^2, \boldsymbol{\mu}_1^2) - \mathcal{D}(\mathbf{z}_i^2, \boldsymbol{\mu}_2^2)| < \varepsilon$, the sample has the same cluster assignment in $\mathbf{Y}_{(t)}$ as that in \mathbf{Y}^1 of the informative views.

Case 2: For any three clusters, e.g., $\boldsymbol{\mu}_1^1, \boldsymbol{\mu}_2^1$, and $\boldsymbol{\mu}_3^1$ in the 1-st view, $\boldsymbol{\mu}_1^2, \boldsymbol{\mu}_2^2$, and $\boldsymbol{\mu}_3^2$ in the 2-nd view, if a sample is noisy in all views, there is no harm in supposing that $\mathcal{D}(\mathbf{z}_i^1, \boldsymbol{\mu}_1^1) \approx \mathcal{D}(\mathbf{z}_i^1, \boldsymbol{\mu}_2^1) < \mathcal{D}(\mathbf{z}_i^1, \boldsymbol{\mu}_3^1)$ and $\mathcal{D}(\mathbf{z}_i^2, \boldsymbol{\mu}_1^2) > \mathcal{D}(\mathbf{z}_i^2, \boldsymbol{\mu}_2^2) \approx \mathcal{D}(\mathbf{z}_i^2, \boldsymbol{\mu}_3^2)$, i.e., $y_{i1}^1 \approx y_{i2}^1 > y_{i3}^1$ and $y_{i1}^2 < y_{i2}^2 \approx y_{i3}^2$. In this situation, the sample is noisy in two views and the common cluster assignments are y_{i2}^1 and y_{i2}^2 for these two views.

First, we can consider this situation $\mathcal{D}(\mathbf{z}_i^1, \boldsymbol{\mu}_1^1) \approx \mathcal{D}(\mathbf{z}_i^1, \boldsymbol{\mu}_2^1)$ and $\mathcal{D}(\mathbf{z}_i^2, \boldsymbol{\mu}_1^2) > \mathcal{D}(\mathbf{z}_i^2, \boldsymbol{\mu}_2^2)$. According to Theorem B.3, we have

$$\begin{aligned}
 \mathcal{D}(\mathbf{z}_i, \mathbf{c}_1) - \mathcal{D}(\mathbf{z}_i, \mathbf{c}_2) &= (w^1)^2 (\mathcal{D}(\mathbf{z}_i^1, \boldsymbol{\mu}_1^1) - \mathcal{D}(\mathbf{z}_i^1, \boldsymbol{\mu}_2^1)) + (w^2)^2 (\mathcal{D}(\mathbf{z}_i^2, \boldsymbol{\mu}_1^2) - \mathcal{D}(\mathbf{z}_i^2, \boldsymbol{\mu}_2^2)) \\
 &\approx (w^2)^2 (\mathcal{D}(\mathbf{z}_i^2, \boldsymbol{\mu}_1^2) - \mathcal{D}(\mathbf{z}_i^2, \boldsymbol{\mu}_2^2)) > 0,
 \end{aligned}$$

which indicates that $y_{i1} < y_{i2}$.

Then, we can consider this situation $\mathcal{D}(\mathbf{z}_i^1, \boldsymbol{\mu}_2^1) < \mathcal{D}(\mathbf{z}_i^1, \boldsymbol{\mu}_3^1)$ and $\mathcal{D}(\mathbf{z}_i^2, \boldsymbol{\mu}_2^2) \approx \mathcal{D}(\mathbf{z}_i^2, \boldsymbol{\mu}_3^2)$. According to Theorem B.3, we have

$$\begin{aligned}
 \mathcal{D}(\mathbf{z}_i, \mathbf{c}_2) - \mathcal{D}(\mathbf{z}_i, \mathbf{c}_3) &= (w^1)^2 (\mathcal{D}(\mathbf{z}_i^1, \boldsymbol{\mu}_2^1) - \mathcal{D}(\mathbf{z}_i^1, \boldsymbol{\mu}_3^1)) + (w^2)^2 (\mathcal{D}(\mathbf{z}_i^2, \boldsymbol{\mu}_2^2) - \mathcal{D}(\mathbf{z}_i^2, \boldsymbol{\mu}_3^2)) \\
 &\approx (w^1)^2 (\mathcal{D}(\mathbf{z}_i^1, \boldsymbol{\mu}_2^1) - \mathcal{D}(\mathbf{z}_i^1, \boldsymbol{\mu}_3^1)) < 0,
 \end{aligned}$$

which indicates that $y_{i2} > y_{i3}$.

Therefore, $y_{i1}^1 \approx y_{i2}^1 > y_{i3}^1, y_{i1}^2 < y_{i2}^2 \approx y_{i3}^2 \Rightarrow y_{i2} > y_{i1}, y_{i2} > y_{i3}$. Although the sample is noisy in the two views, the scaled representation \mathbf{z}_i is informative and its cluster assignment in $\mathbf{Y}_{(t)}$ is consistent with $y_{i2}^1 \in \mathbf{Y}^1$ and $y_{i2}^2 \in \mathbf{Y}^2$. Indeed, y_{i2}^1 and y_{i2}^2 commonly denote the 2-nd cluster, and they are defined as the common cluster assignments existing in these two views. \square

The proofs in the above theorems can be easily extended to the situation of multiple views.

C. Datasets and Implementations

Table 6. The information of the datasets.

Datasets	V views	K clusters	N samples
BDGP, NoisyBDGP	2, 3	5	2,500
DIGIT, NoisyDIGIT	2, 3	10	5,000
COIL, NoisyCOIL	3, 4	10	720
Amazon, NoisyAmazon	3, 4	10	4,790

Table 7. Comparison results of individual views on the datasets.

Datasets	BDGP			DIGIT			COIL			Amazon		
	NoisyBDGP			NoisyDIGIT			NoisyCOIL			NoisyAmazon		
Evaluation metrics	ACC	NMI	ARI	ACC	NMI	ARI	ACC	NMI	ARI	ACC	NMI	ARI
DEC/View 1	0.457	0.291	0.238	0.809	0.789	0.736	0.758	0.783	0.678	0.470	0.325	0.202
DEC/View 2	0.926	0.819	0.824	0.548	0.641	0.454	0.766	0.815	0.687	0.413	0.301	0.182
DEC/View 3	N/A	N/A	N/A	N/A	N/A	N/A	0.735	0.774	0.664	0.372	0.279	0.185
DEC/Noisy view	0.222	0.002	0.000	0.124	0.004	0.000	0.164	0.028	0.002	0.120	0.004	0.000

Datasets. Four datasets and their noisy versions are used in the experiments. To be specific, BDGP (Cai et al., 2012) is a drosophila embryos dataset where each sample contains a 1,750-dimensional visual view and a 79-dimensional textual view. DIGIT (Peng et al., 2019) is a dataset of handwritten arabic numbers in which each sample has two views coming from MNIST and USPS, respectively. COIL (Nene et al., 1996) is a multi-view dataset and the multiple views of one object are captured by the cameras from different visual angles. Amazon (Saenko et al., 2010) consists of the commodity images, such as bicycles, bags, and earphones. The raw samples are RGB images and we obtain the augmented data by rotation, horizontal flip, and color filter to construct the multi-view dataset, where different views of a multi-view data are different samples with the same semantic category. For these four datasets, we randomly sample noise and build an additional view to obtain NoisyBDGP, NoisyDIGIT, NoisyCOIL, and NoisyAmazon, respectively. All image samples are scaled to $32 \times 32 \times 1$ (DIGIT, COIL, NoisyDIGIT, and NoisyCOIL) or $32 \times 32 \times 3$ (Amazon and NoisyAmazon) pixels for reducing the computational burden.

Comparison methods. We compare MvCAN with 9 baselines including DEC (Xie et al., 2016), MVC-LFA (Wang et al., 2019), COMIC (Peng et al., 2019), DMJC (Xie et al., 2020), DIMC-net (Wen et al., 2020), EAMC (Zhou & Shen, 2020), GP-MVC (Wang et al., 2021), DSMVC (Tang & Liu, 2022a), and DSIMVC (Tang & Liu, 2022b).

Implementation. For a fair comparison, we adopt the widely used network architectures as previous works (Xie et al., 2016; Guo et al., 2017; Xie et al., 2020) to implement the deep autoencoders. Concretely, for the vector input (BDGP and NoisyBDGP), the autoencoder adopts the fully connected network with the architecture of $\mathbf{X}^v - 500 - 500 - 2000 - \mathbf{Z}^v - 2000 - 500 - 500 - \hat{\mathbf{X}}^v$. For the image input (DIGIT, COIL, Amazon, NoisyDIGIT, NoisyCOIL, and NoisyAmazon), the autoencoder adopts the convolutional neural network whose architecture is $\mathbf{X}^v - 32 - 64 - 64 - \mathbf{Z}^v - 64 - 32 - 32 - \hat{\mathbf{X}}^v$ with the kernel size of 4×4 , the stride of 2, and the padding of 1. The dimensionality of \mathbf{Z}^v is set to 10. The activation function in networks is ReLU (Glorot et al., 2011). The deep model structure achieves the decoupling of multiple views' network parameters. Adam (Kingma & Ba, 2015) with a learning rate of 0.0001 is adopted for mini-batch optimization with the batch size of 256. Specifically, to make the optimization of multiple views be away from mutual interference, we respectively construct V decoupled Adam optimizers for V different views. In general, the autoencoders are initialized by minimizing the reconstruction loss, and then the model is trained by minimizing the clustering and reconstruction losses for convergence. In \mathcal{T} -level optimization, $T_1 = 2$. In \mathcal{R} -level optimization, $T_2 = 100$.

All experiments are conducted on a Windows PC with NVIDIA GeForce RTX 3090 GPU (24.0GB caches) and 11th Gen Intel(R) Core(TM) i5-11600KF @ 3.90GHz, 64.0GB RAM.

D. Additional Results

Table 8. Importance of two conditions in clustering objective.

	Conditions		BDGP			DIGIT			COIL			Amazon		
	Θ^v	\mathbf{A}^v	ACC	NMI	ARI	ACC	NMI	ARI	ACC	NMI	ARI	ACC	NMI	ARI
(i)	✓		0.973	0.921	0.935	0.986	0.980	0.982	0.942	0.924	0.886	0.795	0.810	0.714
(ii)		✓	0.660	0.477	0.451	0.840	0.735	0.690	0.913	0.868	0.825	0.685	0.696	0.536
(iii)	✓	✓	0.984	0.953	0.961	0.995	0.988	0.989	0.996	0.991	0.990	0.826	0.867	0.779

Table 9. Importance of two conditions in clustering objective.

	Conditions		NoisyBDGP			NoisyDIGIT			NoisyCOIL			NoisyAmazon		
	Θ^v	\mathbf{A}^v	ACC	NMI	ARI	ACC	NMI	ARI	ACC	NMI	ARI	ACC	NMI	ARI
(i)	✓		0.977	0.946	0.949	0.902	0.933	0.884	0.890	0.912	0.851	0.667	0.747	0.621
(ii)		✓	0.602	0.339	0.305	0.611	0.599	0.436	0.806	0.832	0.719	0.523	0.514	0.390
(iii)	✓	✓	0.980	0.951	0.957	0.990	0.984	0.986	0.992	0.988	0.987	0.728	0.732	0.614

Table 10. Importance of two loss components in optimization.

	Components		BDGP			DIGIT			COIL			Amazon		
	\mathcal{L}_r	\mathcal{L}_c	ACC	NMI	ARI	ACC	NMI	ARI	ACC	NMI	ARI	ACC	NMI	ARI
(a)			0.643	0.522	0.245	0.768	0.723	0.635	0.839	0.927	0.838	0.441	0.373	0.268
(b)	✓		0.948	0.842	0.874	0.787	0.747	0.658	0.826	0.888	0.787	0.498	0.452	0.322
(c)		✓	0.798	0.709	0.656	0.870	0.943	0.867	0.876	0.957	0.876	0.724	0.817	0.678
(d)	✓	✓	0.984	0.953	0.961	0.995	0.988	0.989	0.996	0.991	0.990	0.826	0.867	0.779

Table 11. Importance of two loss components in optimization.

	Components		NoisyBDGP			NoisyDIGIT			NoisyCOIL			NoisyAmazon		
	\mathcal{L}_r	\mathcal{L}_c	ACC	NMI	ARI	ACC	NMI	ARI	ACC	NMI	ARI	ACC	NMI	ARI
(a)			0.499	0.315	0.253	0.741	0.705	0.611	0.828	0.875	0.785	0.432	0.371	0.269
(b)	✓		0.944	0.839	0.864	0.769	0.748	0.651	0.813	0.867	0.780	0.487	0.455	0.341
(c)		✓	0.726	0.574	0.381	0.591	0.702	0.504	0.686	0.782	0.612	0.423	0.423	0.258
(d)	✓	✓	0.980	0.951	0.957	0.990	0.984	0.986	0.992	0.988	0.987	0.728	0.732	0.614

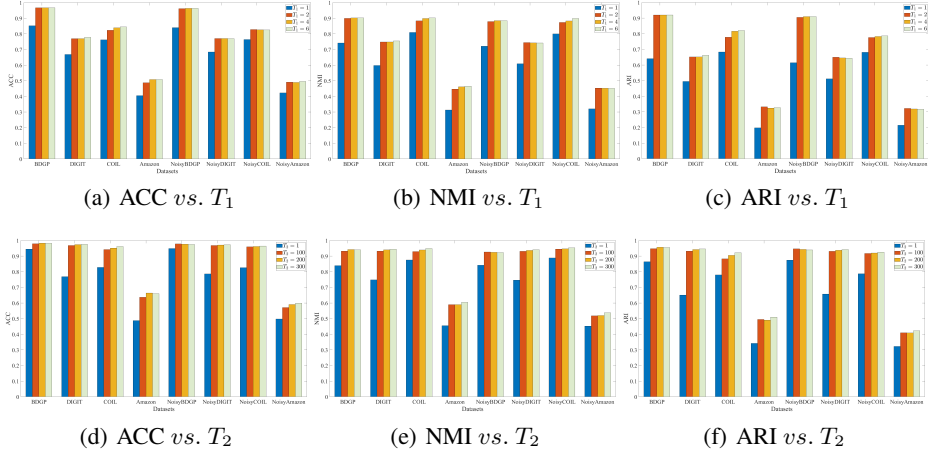

 Figure 7. Change the numbers of T_1 (a-c) and T_2 (d-f) in the proposed bi-level optimization strategy.

Table 8 and Table 9 list the clustering results in terms of two conditions on all datasets. Table 10 and Table 11 list the clustering results in terms of loss components on all datasets. Figure 7 reports the clustering results by changing the numbers of T_1 (a-c) and T_2 (d-f) in the proposed bi-level optimization strategy.

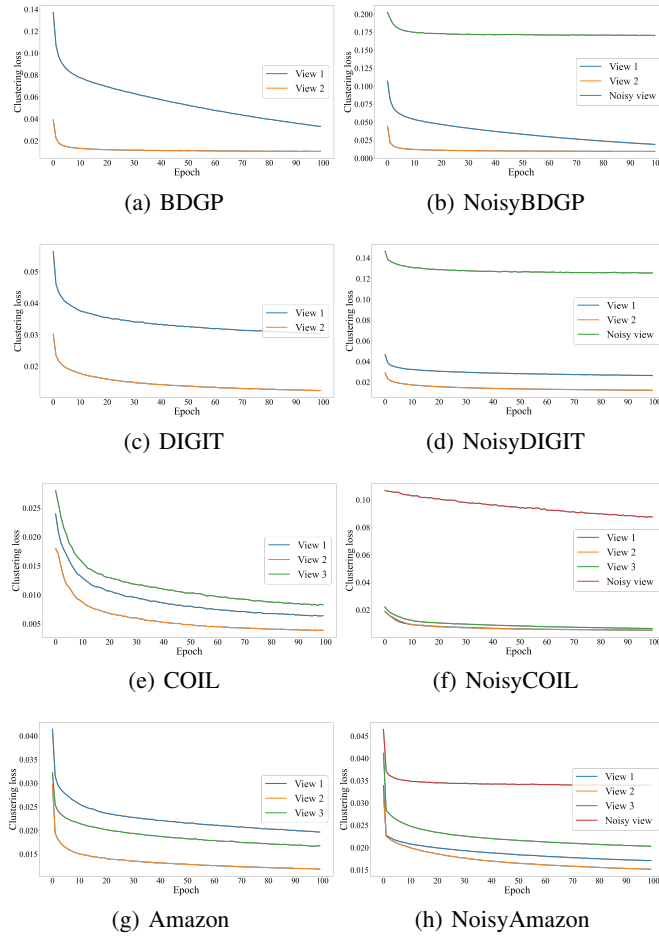


Figure 8. Loss vs. Epoch.

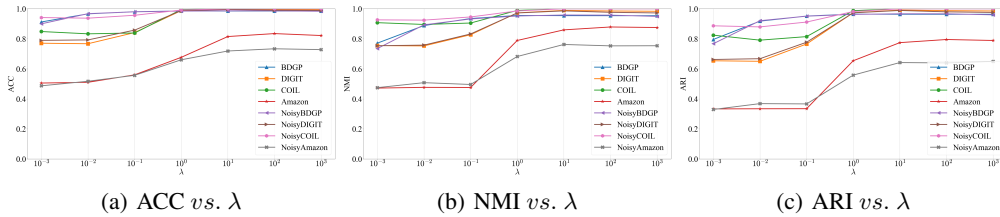


Figure 9. Clustering results vs. λ .

Convergence analysis. Figure 8 plots the clustering loss curve during training on all datasets.

Hyper-parameter analysis. Figure 9 shows the clustering results with different trade-off values. Figure 10 visualizes the representations learned with different prior knowledge of cluster numbers on all datasets.

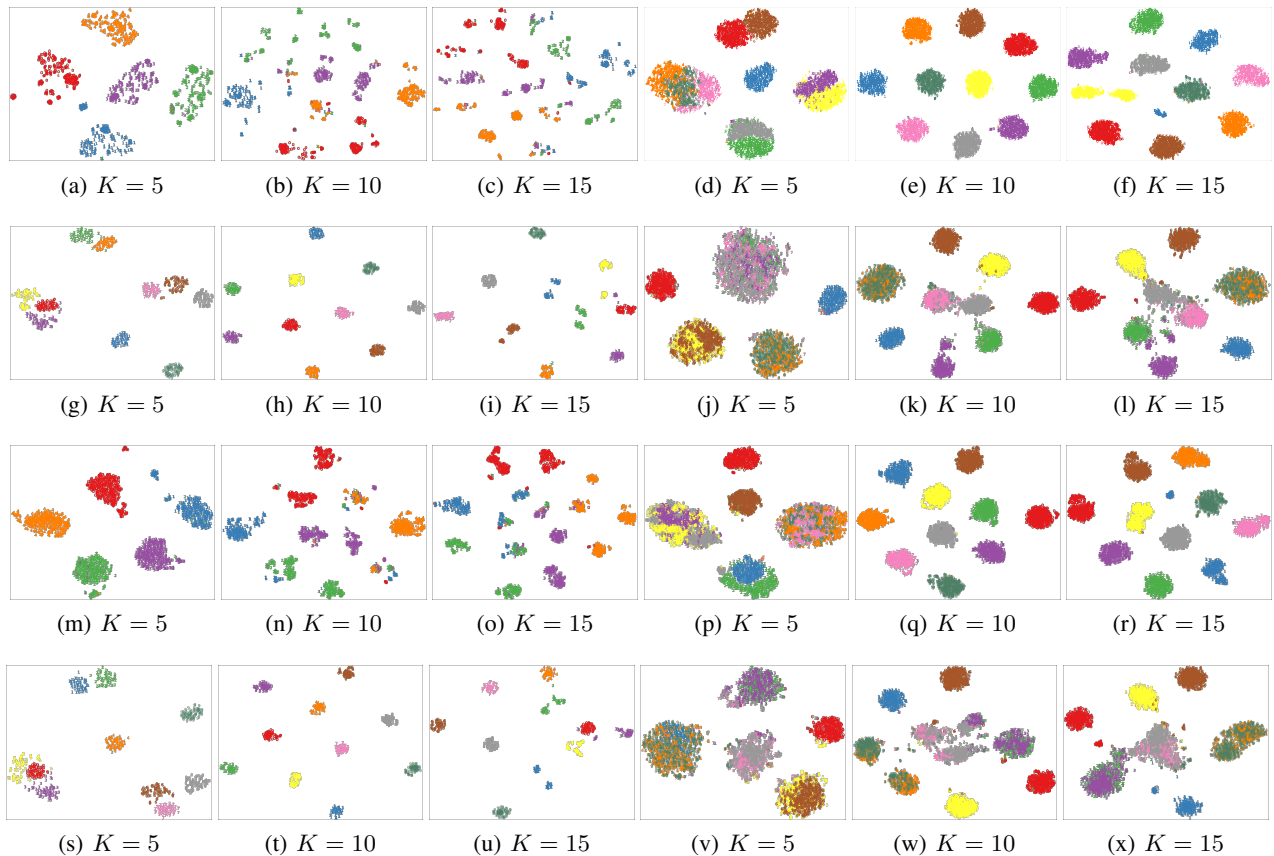


Figure 10. Visualization of the representations learned with different prior knowledge of cluster numbers on all datasets. BDGP (a-c), DIGIT (d-f), COIL (g-i), Amazon (j-l), NoisyBDGP (m-o), NoisyDIGIT (p-r), NoisyCOIL (s-u), NoisyAmazon (v-x).

E. Social Impacts

We expect this work could inspire more applications, such as animal protection and automatic pilot. It might be promising to take the noisy-view drawback (NVD) into account, especially in unsupervised environments where the qualities of different views captured by various sensors cannot be guaranteed, *e.g.*, the views from some sensors are faulty or not applicable and bring noisy information. Additionally, our work proposed a machine learning algorithm to handle the NVD. This research is not expected to introduce new negative societal impacts beyond what is already known.